nature neuroscience

Coordinated memory replay in the visual cortex and hippocampus during sleep

Daoyun Ji & Matthew A Wilson

Sleep replay of awake experience in the cortex and hippocampus has been proposed to be involved in memory consolidation. However, whether temporally structured replay occurs in the cortex and whether the replay events in the two areas are related are unknown. Here we studied multicell spiking patterns in both the visual cortex and hippocampus during slow-wave sleep in rats. We found that spiking patterns not only in the cortex but also in the hippocampus were organized into frames, defined as periods of stepwise increase in neuronal population activity. The multicell firing sequences evoked by awake experience were replayed during these frames in both regions. Furthermore, replay events in the sensory cortex and hippocampus were coordinated to reflect the same experience. These results imply simultaneous reactivation of coherent memory traces in the cortex and hippocampus during sleep that may contribute to or reflect the result of the memory consolidation process.

The hippocampus is essential for episodic memory[1,2]. The dominant theory of system memory consolidation proposes that active communication between the cortex and hippocampus transforms new memory in the hippocampus into long-term memory stored in the cortex[3,4]. Recent studies have provided electrophysiological evidence for the involvement of the hippocampus and neocortex in memory processing during sleep, reflecting either active participation in the process of memory consolidation as proposed in theoretical models[5,6] or reactivation of consolidated memory traces. First, electroencephalogram (EEG) events between the cortex and hippocampus are correlated[7–11], suggesting the two areas are engaged in active interaction during sleep. Second, cell pairs that are correlated during awake experience are also correlated during subsequent sleep within the hippocampus[12–14], within the cortex[15], and between the hippocampus and cortex[16]. These pairwise correlation results and other correlation-based analysis[17] imply that the experience-related neuronal activity is, to some degree, reactivated during sleep. However, the reactivation in these studies lacks the specificity presumably required for episodic memory, which includes a cascade of temporally ordered events encoded by a unique sequence of activation of different neuronal populations within the cortex, within the hippocampus, or both[18,19]. If sleep reactivation is somehow involved in the processing of episodic memory traces, this sequential structure should be specifically replayed. Indeed, replay of specific ensemble-level patterns has been utilized in a detailed model of memory consolidation[6]. Therefore, it is important to experimentally study the more specific high-order replay, in which a temporally sequential firing order across multiple cells is recaptured during sleep. Such high-order replay has been observed in the hippocampus during slow-wave sleep (SWS)[20,21] and rapid-eye-movement sleep[22]. However, whether high-order replay exists in the cortex remains unknown. More importantly, the relationship between replay events in the cortex and hippocampus has not been studied. The present study was designed to address these issues by recording spiking activity in both the visual cortex and the hippocampal CA1 area of rats during active maze-running and during natural sleep (**Fig. 1**). As we examined a primary sensory area that is not explicitly driven by the hippocampus, any observed replay was more likely to reflect broad cortical reactivation not limited to directly hippocampus-driven activity. Four rats were trained to sleep for 1–2 hours (PRE), followed by an awake session (RUN) during which they alternated between two trajectories (leftright and rightleft) on a figure-8 maze, followed by another 1–2 hours sleep session (POST). We found that high-order replay of RUN firing patterns occurred not only in the hippocampus but also in the visual cortex during SWS, and the replays in the two areas were coordinated to represent the same coherent awake experience.

RESULTS

Firing patterns during SWS in the cortex and hippocampus

We first searched for spiking patterns at the population level in the visual cortex and hippocampus during SWS. In the neocortex, cells display active depolarized (up) and silent hyperpolarized (down) states *in vitro*[23–25], in anesthetized animals and during SWS[26–29]. Cortical cells both within and across different cortical regions switch between up and down states synchronously[9,26,27]. In agreement with these previous results, we observed that cells across different layers in the visual cortex displayed synchronized stepwise increases and decreases in multiunit activity during SWS (**Fig. 2a**). More specifically, we observed periods of 80–300 ms during which the entire population of the recorded visual cortical cells were silent. These periods of silence were followed by increases in activity across the population lasting up to a few seconds.

The Picower Institute for Learning and Memory, RIKEN-MIT Neuroscience Research Center, Department of Brain and Cognitive Sciences and Department of Biology, Massachusetts Institute of Technology, Building 46, Room 5233, 43 Vassar Street, Cambridge, Massachusetts 02139, USA. Correspondence should be addressed to M.A.W. (mwilson@mit.edu) or D.J. (dji@mit.edu).

Received 28 June; accepted 30 November; published online 17 December 2006; doi:10.1038/nn1825

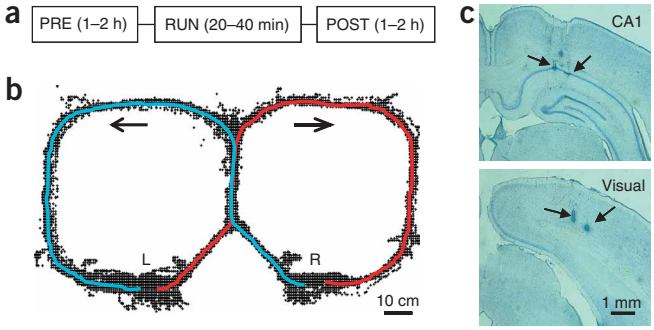

Figure 1 Experimental design. (**a**) On each recording day, there were three recording sessions: a 1–2 hour sleep session (PRE), a 20–40 minute maze-running session (RUN), and another 1–2 hour sleep session (POST) after the run. (**b**) During the RUN sessions, rats were trained to run an alternation task on a figure-8-shaped maze. All the visited position points during a typical RUN session are plotted to show the shape of the maze. Rats had to alternate between the red (leftright) and blue (rightleft) running trajectories to receive a reward at R or L. The arrows mark the running directions. (**c**) We implanted tetrodes to record CA1 cells in the hippocampus and cells in the visual cortex. Histology micrographs show two lesion spots (arrows), which mark the tetrode tip locations, in the CA1 pyramidal cell layer ('CA1'), and two in the deep layers of the primary visual cortex V1 ('visual').

We refer to these active periods as frames. We are using the term 'frame' rather than 'up state' because we identified the phenomenon by changes in multiunit activity rather than EEG rhythms or intracellular potentials, and because similar structure also exists in the hippocampus (see below) where no intrinsic up and down states have been reported. On average, cortical frames occurred at a rate 47.3 ± 2.1 min^{-1} (mean ± s.e.m.) during SWS (n = 20,545 during 20 sleep sessions from four rats). There was no difference in occurrence rate between PRE and POST (PRE, 44.3 ± 3.5 min^{-1}; POST, 49.9 ± 3.3 min^{-1}; P = 0.193, t-test). The frame durations were distributed widely between 0.1 and 3 s with a mean 0.96 s and median 0.67 s, whereas the mean and median durations of the interframe silent periods were 0.17 s and 0.13 s, respectively (**Fig. 2b**). Cortical frames during POST had slightly shorter durations (PRE, mean 1.1 s, median 0.73 s; POST, mean 0.90 s, median 0.65 s; $P = 2.2 \times 10^{-15}$, rank-sum test) and slightly higher within-frame multiunit firing rates per tetrode (PRE, mean 54.5 Hz, median 48.3 Hz; POST, mean 58.7 Hz, median 54.1 Hz; $P = 1.2 \times 10^{-19}$, rank-sum test) than those during PRE. As shown in **Figure 2a**, the interframe silent periods were correlated with positive peaks of EEG K-complexes[28] in layer 5. This observation was confirmed by frame start- and end-time–triggered EEG averages (**Fig. 2c**). On average, the cortical frames ended about 20 ms earlier than the K-complex positive peaks, and they started about 50 ms earlier than the K-complex negative peaks. Because depth-positive EEG events are reliably associated with down states[28,29], the result imply that the interframe silent periods were produced by cortical cells' simultaneous switch to the down state, and that frames were formed when cells rebounded to the active up state.

Whereas up and down states have been observed in neocortical cells, hippocampal cells have not been reported to display such intrinsic states. Despite this, we observed that the hippocampal neuronal population also displayed during SWS synchronized periods of increased and decreased multiunit activity: that is, frame and silent periods (**Fig. 2a**). On average, hippocampal frames occurred at a rate of 41.7 ± 2.9 min^{-1} during SWS (n = 19,189 during 20 sleep sessions from four rats). There was no significant difference in occurrence rate between PRE and POST (PRE, 40.0 ± 4.1 min^{-1}; POST, 43.5 ± 4.1 min^{-1}; P = 0.35, t-test). Hippocampal frames had shorter duration (mean 0.78 s, median 0.50 s, P = 0, rank-sum test) than the cortical frames, and they were separated by longer interframe silent periods (mean 0.50 s, median 0.22 s, P = 0, rank-sum test) (**Fig. 2b**). Like cortical frames, hippocampal frames during POST had slightly (and insignificantly) shorter durations (PRE, mean 0.81 s, median 0.49 s; POST, mean 0.76 s, median 0.50 s; P = 0.41, rank-sum test) and slightly higher multiunit firing rates per tetrode (PRE, mean 63.0 Hz, median 58.1 Hz; POST, mean 67.6 Hz, median 61.5 Hz; P = 0.040, rank-sum test) than those during PRE. Hippocampal frames were correlated with

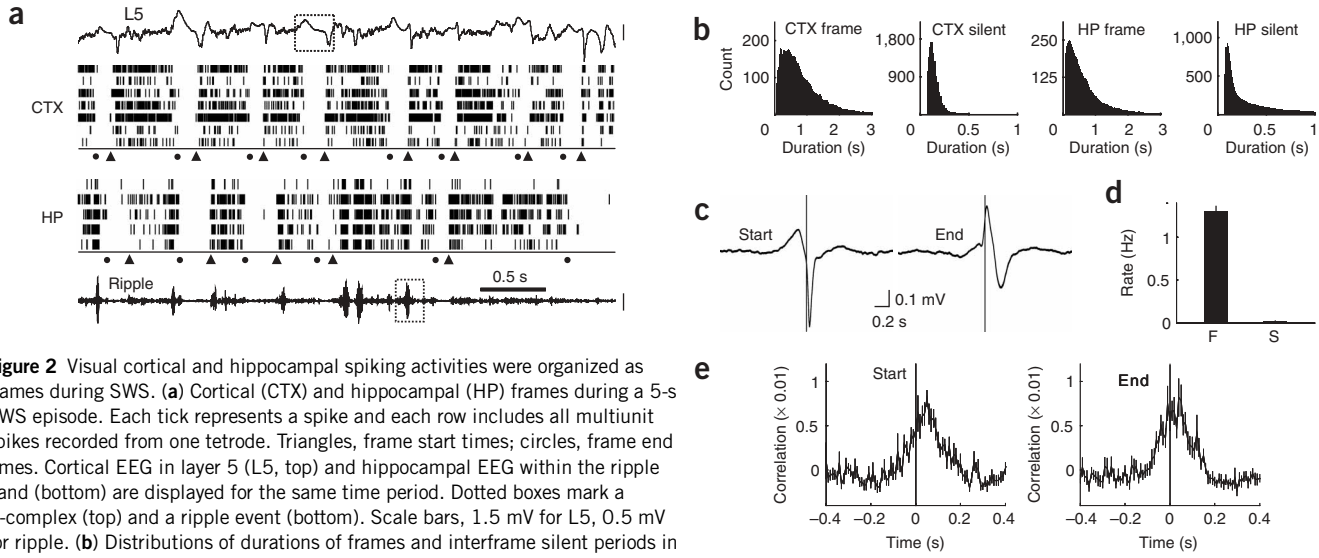

Figure 2 Visual cortical and hippocampal spiking activities were organized as frames during SWS. (**a**) Cortical (CTX) and hippocampal (HP) frames during a 5-s SWS episode. Each tick represents a spike and each row includes all multiunit spikes recorded from one tetrode. Triangles, frame start times; circles, frame end times. Cortical EEG in layer 5 (L5, top) and hippocampal EEG within the ripple band (bottom) are displayed for the same time period. Dotted boxes mark a K-complex (top) and a ripple event (bottom). Scale bars, 1.5 mV for L5, 0.5 mV for ripple. (**b**) Distributions of durations of frames and interframe silent periods in the cortex and hippocampus. (**c**) Cortical EEG averages (mean ± s.e.m., s.e.m. represented by thickness of the curves) triggered by cortical frame start and end times. (**d**) Occurrence rate (mean ± s.e.m., n = 20 sleep sessions) of hippocampal ripple events within hippocampal frames (F) and within interframe silent periods (S). (**e**) Average cross-correlogram (mean ± s.e.m., n = 20 sleep sessions) between cortical and hippocampal frame start times and between their end times. Here the cortex was the reference, meaning a peak at positive time would indicate that the cortex led the hippocampus. Bin size, 10 ms.

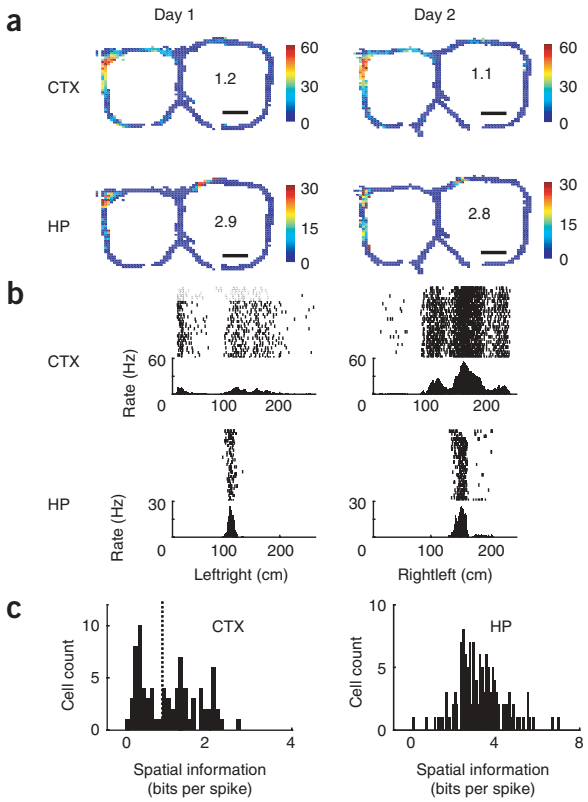

Figure 3 Visual cortical cells displayed localized firing fields. (**a**) Firing rate maps of a cortical cell (CTX) and a hippocampal place cell (HP) on two consecutive recording days. The maze is shown as blue. Color bars, firing rates in Hz; bin size, 2 cm × 2 cm. The number in each map indicates spatial information in bits per spike. Scale bar, 20 cm. (**b**) Consistent firing of the cortical cell and the hippocampal cell examined lap by lap on day 1 when the rat was running the leftright and rightleft trajectories. Each trajectory was linearized and plotted on the *x* axis. In each panel, black dots represent spikes fired at the corresponding positions and one row shows all spikes in one single lap. Laps are arranged top down in increasing temporal order. The bottom histograms represent the binned firing rate computed from the laps shown. Bin size, 2 cm. (**c**) Spatial information from cortical cells and hippocampal cells that were active on the maze. The dashed line indicates the threshold (0.8) used to determine whether a cortical cell had a firing field.

ripples (**Supplementary Fig. 1** online), which are prominent high-frequency (80–250 Hz) oscillation events in the hippocampal EEG[30]. Ripples almost always appeared inside hippocampal frames but not within interframe silent periods (**Fig. 2d**). Individual frames could contain none, one or multiple ripple events (**Supplementary Fig. 1**). Furthermore, ripple events on average started 30 ms later than the frame onsets (**Supplementary Fig. 1**), suggesting ripple events were triggered by frame activity. These results are consistent with the notion that ripple events in the hippocampus were modulated and grouped by the frame structure.

We next studied whether the cortical and hippocampal frames were related. Frame onset and offset times in the visual cortex and hippocampus were significantly correlated (**Fig. 2e**). On average, the cortical frames started about 50 ms earlier ($P = 2.2 \times 10^{-8}$, *t*-test) and ended about 40 ms earlier ($P = 1.0 \times 10^{-5}$) than the hippocampal ones. There was no statistically significant difference in the correlation between PRE and POST, and the temporal relationships were insensitive to parameters that define frame boundaries (**Supplementary Fig. 2** online). However, the broad peaks in the cross-correlograms (**Fig. 2e**) imply that there was no one-to-one correspondence between cortical and hippocampal frames. Therefore, on average, general activity patterns in the cortex and hippocampus were correlated, suggesting active interaction between cortical and hippocampal neuronal ensembles during SWS.

High-order replay in the cortex and hippocampus

To characterize patterned memory reactivation events, we next examined the contents of the cortical and hippocampal frames in relation to the activity evoked by maze-running. Unlike pairwise correlation studies[15,16] (**Supplementary Figs. 3** and **4** online), this study addressed high-order replay by comparing multicell firing sequences generated by running the two trajectories with the firing sequences of the same cells in sleep frames during PRE and POST.

It is well known that hippocampal cells are active in specific places ('place cells'[31]). Place-specific firing has also been reported in the medial entorhinal cortex[32,33], but not in sensory cortices. During RUN, as expected, hippocampal cells fired in their place fields on the maze. Unexpectedly, many cells in the visual cortex (mostly recorded in the deep layers in primary visual cortex (V1) and its surrounding secondary visual cortex), also had localized firing fields (**Fig. 3**). The fields were consistent across days (**Fig. 3a**) as well as across laps within individual RUN sessions (**Fig. 3b**). These spatially localized firing patterns are likely to have resulted from the local visual cues within the maze which provided consistent patterns of visual input, rather than any intrinsic 'place' specificity as seen in hippocampal cells. Using spatial information as a measurement, 54 out of 116 cortical cells were quantified as having localized firing fields on the maze (**Fig. 3c**). Only cells with such firing fields were included in the subsequent analysis. The spatially localized firing fields in the cortex and hippocampus allowed us to establish repeatable multicell firing sequences in both areas during the spatial task (**Fig. 4a**,**b**, lap). Different sequences emerged from different trajectories. We extracted these sequences by assigning numbers (0, 1, etc.) to cells active on a trajectory, and then arranging them according to the order of the cells' peak firing times (**Fig. 4a**,**b**, avg). A sequence generated by a RUN trajectory is referred to as a template sequence. For example, RUN activity patterns in **Figure 4a** gave rise to the template sequence 01234567 when the rat ran the leftright trajectory. We analyzed a total of 12 cortical template sequences across 10 d and four rats. Among three of the four rats, 15 hippocampal template sequences across 8 d were also constructed. In the fourth rat, only two hippocampal place cells recorded were active on the maze, so high-order sequence replay in the hippocampus was not examined in this individual. For each rat, template sequences on the same trajectory were extracted from two or three consecutive recording days. Though these templates may have contained different number of cells, they were likely to have been drawn from the same cell population because the tetrodes were not moved during those days.

To determine whether the template sequences were reexpressed within sleep frames (for example, **Fig. 4a**,**b**, frame), we used a combinatorial method[34]. First, within each frame, a firing sequence was determined by calculating the relative order of peak firing times across the same cells as in a template (**Fig. 4a**,**b**, seq). For example, the frame in **Figure 4a** yielded a sequence 0132567 (the number 4 cell in the template sequence was inactive in this particular frame). We then defined a matching index *I* to measure the similarity between the frame sequence 0132567 and the template sequence 01234567 (see **Supplementary Methods** online for details). Finally, given a matching index *I* we computed the matching probability *p* that a matching index equal to or larger than *I* would be produced by chance, assuming that all possible orders of the same cells are equally probable. The matching

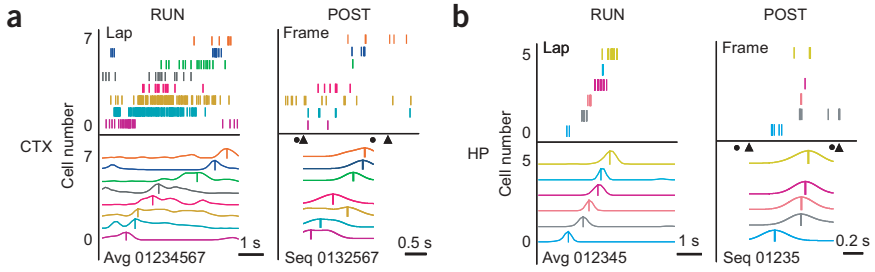

Figure 4 Sleep frames replayed multicell firing sequences during RUN in both the visual cortex and the hippocampus. (**a**) Cortical firing sequence during RUN and in a POST sleep frame. Lap, firing pattern during a single running lap on the leftright trajectory. Each row represents a cell and each tick represents a spike. Avg, template firing sequence obtained by averaging over all laps on the trajectory. Each curve represents the average firing rate of a cell. Cells were assigned to numbers 0, 1, etc. and then arranged (01234567) from bottom to top according to the order of their firing peaks (vertical lines). Frame, the same cells' firing patterns in a POST sleep frame. Triangles and circles, frame start and end times, respectively. Seq, firing sequence in the frame. Spike trains were convolved with a gaussian window and cells were ordered (0132567) according to the peaks (vertical lines) of the resulted curves. (**b**) Same as **a**, but for cells in the hippocampus on the same trajectory.

probability measures the significance of a match between a frame sequence and a template sequence. Unless otherwise specified, we used a threshold $p < 0.05$ to determine whether a sleep frame was a significant match. Such a frame is referred to as a replaying frame. Due to the discrete nature of the matching probability p (see **Supplementary Methods** for details), the exact cutoff threshold depended on the number of cells active in a frame and ranged between 0.028 and 0.049 (**Supplementary Table 1** online). A frame with less than four active cells could not reach this threshold to be considered significant; thus, a replaying frame necessarily contained at least four active cells. For example, both the cortical and the hippocampal frames shown in **Figure 4** were replaying frames. The cortical frame contained the sequence 0132567 with $I = 0.91$ and $p = 0.0014$. The hippocampal frame contained the sequence 01235 with $I = 1$ and $p = 0.0083$. More examples of sequence replays are shown in **Supplementary Figure 5** online.

To compute the overall replay effect, we counted the number of replaying frames out of the total number of candidate frames, defined as those containing at least four active template cells, during SWS within last hour in PRE and within first hour in POST. In the cortex, out of 3,070 PRE and 5,808 POST candidate frames, we identified a total of 163 PRE and 366 POST replaying frames. In the hippocampus, out of 849 PRE and 1,555 POST candidate frames, we identified a total of 39 PRE and 121 POST replaying frames. The ratio between replaying and candidate frame numbers, averaged across all the template sequences, was significantly higher during POST than during PRE in both the cortex (PRE, 0.052 ± 0.008; POST, 0.073 ± 0.009; $P = 0.027$, paired t-test, $n = 12$ templates) and hippocampus (PRE, 0.049 ± 0.011; POST, 0.080 ± 0.007; $P = 0.0057$, $n = 15$ templates). Therefore, in both the cortex and hippocampus, there were significantly more replaying frames during POST than PRE, indicating that the replay was experience dependent. The replaying ratios for every individual template sequence (trajectory) are listed in **Supplementary Table 2** online for cortical templates and in **Supplementary Table 3** online for hippocampal templates. We then investigated the properties of these replay events. First, the ratio in POST decayed back to that of PRE after about 40 min in the cortex (ratio during first 20 min, 0.064 ± 0.011; second 20 min, 0.088 ± 0.013; third 20 min, 0.058 ± 0.009; fourth 20 min, 0.054 ± 0.012), and after about 1 h in the hippocampus (ratio during first 20 min, 0.064 ± 0.006; second 20 min, 0.089 ± 0.012; third 20 min, 0.072 ± 0.017; fourth 20 min, 0.054 ± 0.017). Second, the template sequences were compressed in these replaying events in both the cortex and hippocampus by a similar factor about 5–10 (**Supplementary Fig. 6** online). Third, small differences in frame properties between PRE and POST did not contribute to the observed difference in replaying ratios (**Supplementary Fig. 7** online). Fourth, there was no difference in within-frame multiunit firing rate, within-frame RUN-active-cell firing rate or frame duration between replaying and non-replaying candidate frames (**Supplementary Fig. 8** online). Therefore, the replay identified by the sequence matching method was not biased by differences in these factors between PRE and POST frames.

We then examined whether the observed numbers of replaying frames significantly deviated from those expected by chance, using two methods to evaluate the significance. First, we computed the theoretical distribution of replaying frame numbers by assuming a binomial process in which every frame independently matches a template sequence at the same probability as the cutoff threshold. This distribution is referred to as chance distribution. We compared the observed numbers of replaying frames with those expected from the chance distribution (**Fig. 5a,b**). For all the trajectories combined, the observed numbers in the visual cortex were statistically significant in both POST ($n = 366$, $P < 1 \times 10^{-38}$) and PRE ($n = 163$, $P = 1.4 \times 10^{-6}$). In the hippocampus, the observed numbers were significant in POST ($n = 121$, $P = 8.1 \times 10^{-12}$), but not in PRE ($n = 39$, $P = 0.16$). We repeated the analysis for each individual rat. In the cortex, the observed replaying frame numbers during POST were significant for all four rats (rat 1, $P = 5.0 \times 10^{-11}$; rat 2, $P = 2.8 \times 10^{-11}$; rat 3, $P = 0.00031$; rat 4, $P = 0.0028$), whereas the numbers during PRE were significant for two rats (rat 1, $P = 1.4 \times 10^{-5}$; rat 4, $P = 0.00041$), close to being significant for another (rat 3, $P = 0.067$) and not significant for the last (rat 2, $P = 0.50$). In the hippocampus, the numbers for all three rats were significant in POST (rat 1, $P = 0.0017$; rat 2, $P = 1.5 \times 10^{-7}$; rat 3, $P = 0.00019$), but not in PRE (rat 1, $P = 0.17$; rat 2, $P = 0.52$; rat 3, $P = 0.12$). The second method tested the null hypothesis that a RUN template sequence is replayed with the same probability as any of its

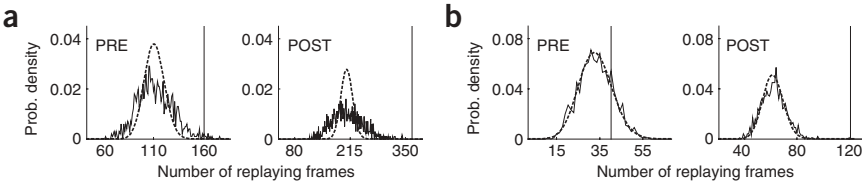

Figure 5 Frame replays occurred significantly more often than chance in POST in both the visual cortex and hippocampus. (**a**) Chance (dotted line) and shuffle (solid line) distributions of the number of replaying frames that were randomly generated for the visual cortex during PRE and POST. Vertical lines, the actual observed numbers of replaying frames. (**b**) Same as **a**, but for the hippocampus.

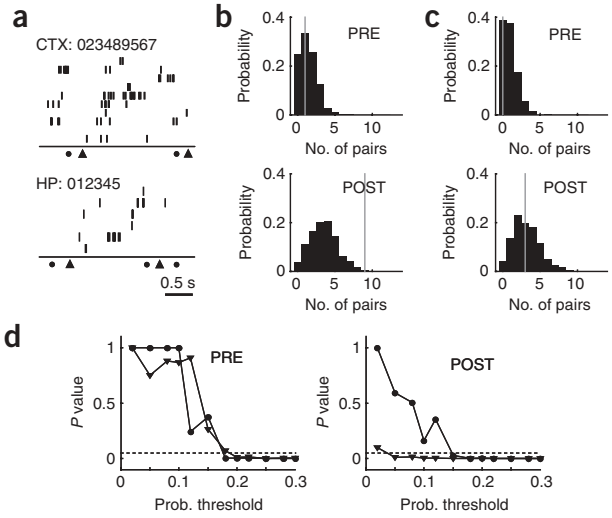

Figure 6 Visual cortical and hippocampal frames that replayed the same trajectories tended to occur at the same time. (**a**) A cortical (CTX) and a hippocampal (HP) replaying frame that overlapped in time. Each row represents a cell and each tick represents a spike. Triangles and circles, frame start and end times, respectively. The two frames replayed the same rightleft trajectory. (**b**,**c**) Distributions of pair numbers produced by shuffling for overlapping cortical-hippocampal frame pairs that replayed the same (**b**) and different (**c**) trajectories in PRE and POST. Vertical gray lines, actual observed numbers. (**d**) Dependence of the significance *P* values of the actual observed numbers on the matching probability threshold in PRE and POST. Lines with filled triangles, same-trajectory; lines with filled circles, different-trajectory; dotted horizontal lines, significance level $P = 0.05$.

random shuffles. From the null hypothesis, a shuffle distribution of replaying frame number was obtained. Against this shuffle distribution, the observed numbers of replaying frames in the visual cortex were also significant (**Fig. 5a**,**b**) in both POST ($P < 0.001$) and PRE ($P = 0.009$), whereas in the hippocampus the numbers were only significant in POST ($P < 0.001$), not in PRE ($P = 0.19$). These analyses verify that replaying frames in POST did not arise from chance. Thus, the sequence-matching analysis demonstrates that a significant number of sleep frames replayed running-evoked firing sequences in both the visual cortex and hippocampus, providing the first direct evidence for high-order replay in the neocortex.

Interaction between cortical and hippocampal replays

To study the interaction between the cortical and hippocampal replays, we next asked whether the replaying frames in the two areas were independent of each other. As we identified only a relatively small number of frames as replaying among a large number of total sleep frames (see numbers above), replaying frames were sparsely distributed during SWS. As a result, the chance that a cortical replaying frame and a hippocampal replaying frame would occur together would be very small if replaying frames in the two areas were not temporally related. We identified replaying cortical and hippocampal frame pairs that matched the same trajectory and overlapped in time ('same-trajectory'). An example of such a pair is shown in **Figure 6a**. The cortical frame had a sequence 023489567 with a matching probability $p = 0.0063$, and the overlapping hippocampal frame had a sequence 012345 with $p = 0.0014$. From the three rats in which both cortical and hippocampal templates were available on the same trajectory, a total of nine such pairs were observed in POST (rat 1, three; rat 2, two; rat 3, four) whereas only one was observed in PRE. As a control comparison, we also counted overlapping frame pairs in which the cortical frame replayed one trajectory while the hippocampal frame replayed the other on the same day ('different-trajectory'). In this case, we observed only three pairs in POST and none in PRE (rat 1, zero; rat 2, two; rat 3, one). We then evaluated the significance of the observed overlapping pairs by comparing the numbers with those expected from the null hypothesis that the replaying frames in the two areas are independent. For this purpose, we applied a shuffling procedure in which replaying frames in the cortex and hippocampus were randomly and independently redistributed among all the candidate frames (**Supplementary Fig. 9** online). We compared the actual observed numbers with distribution of the shuffling-produced overlapping pair numbers (**Fig. 6b**,**c**). The significance level (*P* value) was defined as the number of shuffles that yielded the same or more overlapping pairs than the actual observed pairs divided by the total number of shuffles. In the case of same-trajectory, the observed number of pairs was significant in POST ($P = 0.01$) but not in PRE ($P = 0.75$). For different-trajectory, the observed numbers were not significant in either POST ($P = 0.59$) or PRE ($P > 0.99$). This result indicates that frames in the visual cortex and hippocampus that replayed the same trajectories overlapped more than chance.

The observed number of overlapping replaying pairs was low. However, because only a small fraction of cells that would actually be participating in replay events were recorded, many more frames could be replaying but not detected because of the limited number of cells available. To investigate how robust the overlapping effect was, we varied the matching probability (p) threshold that defines replaying frames. As the threshold increased, we found more overlapping replaying pairs in POST and the number of pairs in POST became statistically significant for a large range of p threshold in the case of same-trajectory (**Fig. 6d**). For example, at the more relaxed

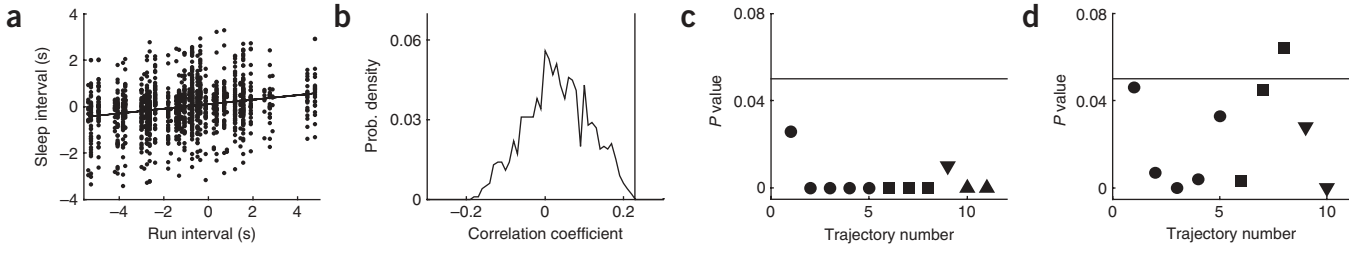

Figure 7 Cortical and hippocampal frames co-replayed the same running trajectory as revealed by interval analysis. (**a**) Time intervals between cortical and hippocampal cell pairs based on cortical replaying frames, compared with their corresponding RUN intervals on a trajectory. Solid line, linear regression between the sleep and RUN intervals. (**b**) Distribution of shuffling-produced correlation. Vertical line, actual observed correlation. (**c**) *P* values of the actual observed correlations based on cortical replaying frames for all trajectories. Trajectories represented by the same shape were from the same rat. Horizontal lines, significance level $P = 0.05$. (**d**) Same as **c**, but based on hippocampal replaying frames.

threshold $P < 0.12$, we found 25 same-trajectory pairs in POST ($P = 0.004$) and only 3 in PRE ($P = 0.91$), whereas for different-trajectory pairs we found 11 in POST ($P = 0.35$) and 5 in PRE ($P = 0.24$). When the threshold became too large (>0.18), the differences between PRE and POST and between same- and different-trajectory were eventually lost. This analysis demonstrates that the overlapping effect was robust and did not depend on a particular choice of matching probability threshold.

To provide further evidence that the replays in the hippocampus and the cortex were coordinated, we applied an interval analysis as follows. For a cell in a replaying frame in one area and a cell in one of its overlapping frames in the other area, we computed the temporal interval between their peak firing times in their corresponding frames, and compared it with the temporal interval between their peak firing times on a RUN trajectory. Based on all cortical replaying frames for a trajectory (as results were similar if replaying frames in PRE and POST were computed separately (data not shown), we combined all the replaying frames in PRE and POST), we first collected sleep intervals of all cell pairs with one cell in a cortical replaying frame and the other in one of its overlapping hippocampal frames (not necessarily replaying), and their corresponding RUN intervals on the trajectory. We then examined whether the sleep intervals and the RUN intervals were correlated. For 11 out of 11 trajectories from four rats, sleep intervals based on cortical replaying frames were significantly correlated with their RUN intervals ($P \leq 0.033$, Pearson's r) (for example, **Fig. 7a**: $r = 0.23$, $P = 1.7 \times 10^{-17}$). Significant correlation could be a result of systematic temporal bias of hippocampal cells or cortical cells on a trajectory or of overall relationship between hippocampal frames and cortical frames (as shown in **Fig. 2e**). To control for this possibility, we shuffled cell identities in the template sequence for the replaying frames and obtained a distribution of correlation from the shuffled templates. We then compared the actual observed correlation with the distribution. For the trajectory shown in **Figure 7a**, the actual observed correlation (0.23) was significantly higher than those produced by the shuffling ($P < 0.001$, **Fig. 7b**). The same was true for all 11 trajectories examined ($P \leq 0.035$, **Fig. 7c**). Similarly, we also performed the analysis based on all the hippocampal replaying frames. In this case, for nine out of ten trajectories from three rats, the correlations between sleep and RUN intervals were significantly higher than those produced by the shuffling ($P \leq 0.048$, **Fig. 7d**). This interval analysis result indicates that, if a frame in the cortex or hippocampus replayed a trajectory, cells in its overlapping frames in the other area fired at the relative temporal interval predicted from the RUN template. Together with the result that frames replaying the same trajectory in the two areas tended to appear simultaneously, the data provide evidence that the fine details of replaying events seem to match coherently the same awake experience in the two areas.

DISCUSSION

Current theory proposes that active interaction between the cortex and hippocampus during offline periods, such as sleep, plays an important role in memory consolidation[5,6]. Here we have described two types of interaction between the neocortical and hippocampal spiking activities during SWS. First, both visual cortical and hippocampal activity patterns seem to be organized into periods of elevated activity referred to as frames. These frames tend to start and end together at a fine time scale, with hippocampal frames briefly lagging cortical frames. Second, at the level of detailed activity pattern, both visual cortical and hippocampal frames replay the multicell firing sequences evoked by awake experience, and the replay in the two areas tends to reflect the same experience (in this case the same trajectory).

Cortical cells switch between up and down state in a synchronized manner during SWS[9,26,27]. This has been described as the cortical slow oscillation in intracellular membrane potential[35,36], and is also seen in the EEG[10,11,37]. We have characterized the extracellular multiunit activity pattern (frame) that presumably arises from such intracellular events. In measurements of similar alternating active and silent periods of individual cortical cells[27], the silent period duration is comparable with that in our data, whereas the active period length is shorter than the frame duration that we measured. This is consistent with the observation that cortical cells are not perfectly synchronized in switching to up state[25–27]. The correlation of cortical frames with K-complexes, a major component of the slow oscillation[28,36], and concurrence of the cortical frame occurrence rate (0.8 Hz) with the slow oscillation frequency range further imply a direct relationship between cortical frames and the slow oscillation. Although these findings indicate that frames may be equivalent to the slow oscillation of cortical cells, the frame structure is also observed in the hippocampus, even though general EEG events are distinctly different. The fact that cortical frames led hippocampal frames by about 50 ms indicates that hippocampal frames may be the result of cortical drive rather than intrinsic state change. Recently, hippocampal interneurons have been found to be phase-locked to cortical up and down state transitions[38], indicating that the frame structure in the hippocampus may be primarily driven or shaped by the interneuron activity. It has also recently been found that slow oscillation in the EEG can be seen in the hippocampus and that the cortical slow EEG oscillation leads the hippocampal one by a similar interval (56 ms)[11]. Thus, it is possible that the slow oscillation reflects or underlies the emergence of the frame structure in both areas. Therefore, frames may serve as basic functional processing units during SWS in many brain areas, and may provide a framework for studying cortical-hippocampal interactions involved in memory consolidation.

Consolidation of episodic memory presumably requires or results in replay of specific neuronal patterns that encode the temporally sequential events in an episode. We have demonstrated that such high-order replay not only occur in the hippocampus but also in the primary visual cortex. The replay implies that specific activity patterns of those cells involved in visual perception (during maze-running) are reactivated during sleep, even if no visual stimuli are present. This is consistent with imaging studies showing that early visual cortices are activated during mental imagery[39] and memory recall[40] in the absence of visual input. Furthermore, the replay also raises the possibility that even early sensory cortices may be involved in memory consolidation, long-term memory storage or both. It has been proposed that episodic memory may be stored distributedly with components involving a particular sensory modality stored in that sensory cortex[41]. Our study is consistent with this hypothesis.

Our data provide evidence that there may be a difference between the hippocampal and cortical replays. In this experiment, we studied memory reactivation only after the memory was well-formed. Therefore, it is quite possible that we observed events that resulted from earlier consolidation[42]. But even for well-trained rats, replays were enhanced by the running experience between PRE and POST sleep in both the cortex and the hippocampus, demonstrating the experience dependence of both cortical and hippocampal replays. During PRE, however, replaying frames already seemed to occur significantly more often than chance in the cortex, but not in the hippocampus. By contrast, the interval analysis result showed that when a cortical replaying frame occurred, during either PRE or POST, hippocampal cells were biased to fire at the same time at locations consistent with those in RUN, meaning that on average there was some degree of reactivation in hippocampal frames that overlapped with cortical

replaying frames; however, the robustness of high-order hippocampal replay was reduced during PRE. In contrast, PRE cortical frames showed a more robust high-order replay, indicating that in well-trained rats cortical memory traces expressed during SWS may be more likely to reflect past RUN experience than hippocampal traces are. This observation is consistent with the theoretical hypothesis that the cortex and hippocampus play complementary roles in memory formation and storage[43,44], with the cortex reflecting long-term memory and the hippocampus reflecting new short-term memory.

We found that the cortical and hippocampal replays were coordinated to match the same awake experience during SWS. The coordination is likely to require active communication between the cortex and hippocampus. The observation that cortical frame onset times precede hippocampal ones (**Fig. 2e**) implies an initial feed-forward interaction from the cortex to hippocampus. However, it remains unclear which area is responsible for initiating individual replay events after frame onsets. Although our data revealed a trend toward hippocampal replays leading those in the neocortex (**Supplementary Fig. 10** online), we were unable to definitively establish the direction of interaction.

Overall, these findings are consistent with a bidirectional interaction model. First, cortical frame activation during SWS biases hippocampal activity and triggers the start of hippocampal frames through cortical-hippocampal projections[45]. This could establish the context or initial conditions for subsequent replay within hippocampal frames. Sequence memories are then reactivated during ripple events that occur within hippocampal frames. The replayed sequence memories are sent back to the associational and then primary sensory cortices through hippocampal-cortical back projections[46], and this biases the cortical activity toward simultaneous cortical frame replay which gradually strengthens cortical-cortical synapses for long-term memory storage. In this model, the two-way interaction and memory trace transfer occur within individual hippocampal and cortical frames. Indeed, there is evidence that neuronal activity propagates among cortical layers[25] and among cortical areas[26,27] under broad synchrony of up state activation. The expression of these reactivated memory traces in sensory cortex may directly relate to the perceptual imagery experienced during sleep and dream states.

METHODS

Rats and experimental procedures. Four Long-Evans rats (5–8 months old) were trained to sleep in a sleep box and run an alternation task on a figure-8-shaped maze (**Fig. 1**). The daily training procedure was exactly same as in later recording days. Intra-maze cues, such as black and white stripes with different orientations and simple geometric shapes, were added to the maze floors and inner walls. The entire maze was surrounded by a black curtain without obvious distal cues except for the irregular wrinkles of the curtain. The rats were trained to alternate between two running trajectories (leftright and rightleft) to get food at two reward sites. The training and later recording protocol was approved by the Committee on Animal Care at Massachusetts Institute of Technology and followed US National Institutes of Health guidelines.

After about 2–3 weeks' training, we implanted on the rat's skull a microelectrode array containing 18 independently adjustable tetrodes. Six to eight tetrodes were assigned to the hippocampus (anteroposterior –3.9, mediolateral 2.2, relative to bregma) and 10–12 tetrodes aimed at primary visual cortex (anteroposterior –7.1, mediolateral 3.5). We inserted a bipolar electrode into the rat's neck muscle to record the electromyogram (EMG). We reintroduced rats to the maze one week after the surgery and retrained them for about 10–15 d before the recording. Recording began once units were stable and rats ran each trajectory at least 20 times. This study only includes data taken from well-trained rats (alternation with at least 80% accuracy). Spikes from tetrodes with any of the four channels crossing a preset triggering threshold were acquired at 32 kHz. EMG and EEG signals were filtered at 0.1–475 Hz and recorded continuously at 2 kHz. Two infrared diodes were used to track the rat's position during a RUN session. Diode positions were sampled at 30 Hz with a resolution of approximately 0.67 cm. On some days, diodes were mounted not directly over but on one side of the rat's head, causing one loop of the maze to appear slightly smaller than the other.

Data analysis. We used ten datasets (two or three consecutive days per rat), each of which contained at least ten RUN-active visual cortical cells and ten RUN-active hippocampal cells, in this analysis. In total, we recorded 116 cortical cells and 294 CA1 cells. Among them, 97 cortical cells (RUN mean rate $\geq$ 0.5 Hz) and 129 CA1 place cells (RUN mean rate $\geq$ 0.2 Hz and $<$ 4 Hz) were active on the maze. Most of the cortical cells were located in the deep layers (5 or 6) in primary visual cortex (V1). A few cells were recorded from layers 4 and 3 in V1 and some other cells from deep layers of the visual cortical area immediately lateral to V1. Tetrode locations were identified according to ref. 47.

Sleep stage classification. EMG, hippocampal and cortical EEGs were used to classify sleep states at 1-s resolution into four stages: wake state, SWS, rapid-eye-movement sleep and an unspecified intermediate state (**Supplementary Fig. 11** online). SWS was characterized as having low EMG, high hippocampal ripple, low hippocampal theta and high cortical delta power[48].

Frame definition. All multiunit spikes (not necessarily sorted single-unit spikes) from all tetrodes within the same recording area were used to determine frame boundaries (see **Supplementary Fig. 12** online for details). Spikes from a recording area were combined and counted in 10 ms time bins. Spike counts were then smoothed using a gaussian window with $\sigma = 30$ ms. Interframe silent periods were defined as periods with spike counts below a preset threshold, and frames as periods in between. Furthermore, consecutive frames with a gap shorter than a threshold were combined.

Frame-triggered EEG and ripple detection. Broadband (0.1–475 Hz) EEGs recorded in layer 5 were used for cortical frame-triggered averages. For the hippocampus, EEGs recorded from the CA1 pyramidal cell layer were first filtered for ripple band (80–250 Hz), and then ripple power was calculated as squared EEG value at each time point. For a selected time point (start or end time) of a frame, a 5-s EEG (or EEG power) segment centered at the time was selected. All the segments triggered by all frames in consideration were then averaged to obtain the mean trace. Ripple events were detected using a threshold-crossing method on the filtered hippocampal EEG at ripple band[7,30]. Two thresholds were defined. If S is the standard deviation of an EEG trace, 3S was set as cross-threshold and 7S as peak-threshold. All the time points with absolute EEG values larger than the cross-threshold were identified. Time points separated by gaps smaller than 50 ms were grouped as a single event. Furthermore, only events with a peak absolute value larger than the peak-threshold were taken as ripple events and the peak time was considered to be the ripple event time. The method also determined the start and end times for every ripple event.

Frame cross-correlation. Frame start (or end) times were treated as discrete events. We first converted the events to occurrence rates with a bin size 10 ms. Given two event rates $f_1(t)$ and $f_2(t)$, where $t = 1,2,\ldots,n$, the cross-correlation coefficient at time lag Δt between the two events was computed as

$$C_{12}(\Delta t) = \frac{\sum_{t=1}^{n} (f_1(t) - \overline{f_1})(f_2(t+\Delta t) - \overline{f_2})}{\sqrt{\sum_{t=1}^{n} (f_1(t) - \overline{f_1})^2}\sqrt{\sum_{t=1}^{n} (f_2(t) - \overline{f_2})^2}},$$

where

$$\overline{f_i} = \frac{1}{n}\sum_{t=1}^{n} f_i(t), \quad \text{for } i = 1, 2.$$

As the correlation coefficient is normally distributed if we assume a null hypothesis that two events are independent Poisson processes[49], we used a t-test to test the dependence between two event trains at a time lag.

Firing rate map and spatial information. Position points on the maze were binned into 2-cm × 2-cm grids. A firing rate map was obtained by simply counting a cell's spikes in a grid divided by the rat's total occupancy time in it.

Only position points and spikes during trajectory running were included. Spatial information was computed using one-dimensional linearized trajectories instead of the two-dimensional maze. The two trajectories (leftright and rightleft) were linearized separately, binned with 2-cm bins, and then combined. The cell's firing rate in each bin of the two linearized trajectories was computed similarly to that of the two-dimensional maze by counting spikes divided by occupancy time. If f_i, t_i ($i = 1,2,\ldots,n$) are the firing rate and occupancy time for the i^{th} bin, spatial information is given by[50]

$$SpI = \sum_{i=1}^{n} p_i \frac{f_i}{f} \log_2 \frac{f_i}{f},$$

where

$$p_i = t_i / \sum_i t_i$$

is the occupancy probability and

$$f = \sum_i p_i f_i$$

is the mean firing rate.

Sequence matching and interval analysis. Sequence construction, sequence similarity, sequence matching probability, overall replay significance, overlapping frame pairs and overlapping significance, and interval analysis are briefly described in the Results section. See **Supplementary Methods** for more details.

Note: Supplementary information is available on the Nature Neuroscience website.

ACKNOWLEDGMENTS

We thank E. Miller, C. Moore, J. Fisher and F.-M. Zhou for critical readings on the manuscript, and Wilson laboratory members for technical help and suggestions and comments on the project and manuscript. Supported by grants to M.A.W. from the Brain Science Institute at the Institute of Physical and Chemical Research (RIKEN) in Japan and the US National Institutes of Health.

COMPETING INTERESTS STATEMENT

The authors declare that they have no competing financial interests.

Published online at http://www.nature.com/natureneuroscience
Reprints and permissions information is available online at http://npg.nature.com/reprintsandpermissions/

1. Squire, L.R. Memory and the hippocampus: a synthesis from findings with rats, monkeys, and humans. *Psychol. Rev.* **99**, 195–231 (1992).
2. Fortin, N.J., Agster, K.L. & Eichenbaum, H.B. Critical role of the hippocampus in memory for sequence of events. *Nat. Neurosci.* **5**, 458–462 (2002).
3. Squire, L.R., Stark, C.E. & Clark, R.E. The medial temporal lobe. *Annu. Rev. Neurosci.* **27**, 279–306 (2004).
4. Hasselmo, M.E. & McClelland, J.L. Neural models of memory. *Curr. Opin. Neurobiol.* **9**, 184–188 (1999).
5. Alvarez, P. & Squire, L.R. Memory consolidation and the medial temporal lobe: a simple network model. *Proc. Natl. Acad. Sci. USA* **91**, 7041–7045 (1994).
6. Káli, S. & Dayan, P. Off-line replay maintains declarative memories in a model of hippocampal-neocortical interactions. *Nat. Neurosci.* **7**, 286–294 (2004).
7. Siapas, A.G. & Wilson, M.A. Coordinated interactions between hippocampal ripples and cortical spindles during slow-wave sleep. *Neuron* **21**, 1123–1128 (1998).
8. Sirota, A., Csicsvari, J., Buhl, D. & Buzsáki, G. Communication between neocortex and hippocampus during sleep in rodents. *Proc. Natl. Acad. Sci. USA* **100**, 2065–2069 (2003).
9. Battaglia, F.P., Sutherland, G.R. & McNaughton, B.L. Hippocampal sharp wave bursts coincide with neocortical up-state transitions. *Learn. Mem.* **11**, 697–704 (2004).
10. Mölle, M., Yeshenko, O., Marshall, L., Sara, S.J. & Born, J. Hippocampal sharp wave-ripples linked to slow oscillations in rat slow-wave sleep. *J. Neurophysiol.* **96**, 62–70 (2006).
11. Wolansky, T., Clement, E.A., Peters, S.R., Palczak, M.A. & Dickson, C.T. Hippocampal slow oscillation: a novel EEG state and its coordination with ongoing neocortical activity. *J. Neurosci.* **26**, 6213–6229 (2006).
12. Wilson, M.A. & McNaughton, B.L. Reactivation of hippocampal ensemble memories during sleep. *Science* **265**, 676–679 (1994).
13. Skaggs, W.E. & McNaughton, B.L. Replay of neuronal firing sequences in rat hippocampus during sleep following spatial experience. *Science* **271**, 1870–1873 (1996).
14. Kudrimoti, H.S., Barnes, C.A. & McNaughton, B.L. Reactivation of hippocampal cell assemblies: effects of behavioral state, experience, and EEG dynamics. *J. Neurosci.* **19**, 4090–4101 (1999).
15. Hoffman, K.L. & McNaughton, B.L. Coordinated reactivation of distributed memory traces in primate neocortex. *Science* **297**, 2070–2073 (2002).
16. Qin, Y.L., McNaughton, B.L., Skaggs, W.E. & Barnes, C.A. Memory reprocessing in corticocortical and hippocampocortical neuronal ensembles. *Phil. Trans. R. Soc. Lond. B* **352**, 1525–1533 (1997).
17. Ribeiro, S. *et al.* Long-lasting novelty-induced neuronal reverberation during slow-wave sleep in multiple forebrain areas. *PLoS Biol.* **2**, 24 (2004).
18. Eichenbaum, H., Dudchunko, P., Wood, E., Shapiro, M. & Tanila, H. The hippocampus, memory, and place cells: is it spatial memory or a memory space? *Neuron* **23**, 209–226 (1999).
19. Jensen, O. & Lisman, J.E. Hippocampal sequence-encoding driven by a cortical multi-item working memory buffer. *Trends Neurosci.* **28**, 67–72 (2005).
20. Nádasdy, Z., Hirase, H., Czurkó, A., Csicsvari, J. & Buzsáki, G. Replay and time compression of recurring spike sequences in the hippocampus. *J. Neurosci.* **19**, 9497–9507 (1999).
21. Lee, A.K. & Wilson, M.A. Memory of sequential experience in the hippocampus during slow wave sleep. *Neuron* **36**, 1183–1194 (2002).
22. Louie, K. & Wilson, M.A. Temporally structural replay of awake hippocampal ensemble activity during rapid eye movement sleep. *Neuron* **29**, 145–156 (2001).
23. Cossart, R., Aronov, D. & Yuste, R. Attractor dynamics of network up states in the neocortex. *Nature* **423**, 283–288 (2003).
24. Shu, Y., Hasenstaub, A. & McCormick, D.A. Turning on and off recurrent balanced cortical activity. *Nature* **423**, 288–293 (2003).
25. Sanchez-Vives, M.V. & McCormick, D.A. Cellular and network mechanisms of rhythmic recurrent activity in neocortex. *Nat. Neurosci.* **3**, 1027–1034 (2000).
26. Petersen, C.C., Hahn, T.T.G., Metha, M., Grinvald, A. & Sakmann, B. Interaction of sensory responses with spontaneous depolarization in layer 2/3 barrel cortex. *Proc. Natl. Acad. Sci. USA* **100**, 13638–13643 (2003).
27. Volgushev, M., Chauvette, S., Mukovski, M. & Timofeev, I. Precise long-range synchronization of activity and silence in neocortical neurons during slow-wave sleep. *J. Neurosci.* **26**, 5665–5672 (2006).
28. Amzica, F. & Steriade, M. Cellular substrates and laminar profile of sleep K-complex. *Neuroscience* **82**, 671–686 (1998).
29. Steriade, M., Timofeev, I. & Grenier, F. Natural waking and sleep states: a view from inside neocortical neurons. *J. Neurophysiol.* **85**, 1969–1985 (2001).
30. Csicsvari, J., Hirase, H., Mamiya, A. & Buzsáki, G. Ensemble patterns of hippocampal CA3-CA1 neurons during sharp wave-associated population events. *Neuron* **28**, 585–594 (2000).
31. O'Keefe, J. & Dostrovsky, J. The hippocampus as a spatial map: preliminary evidence from unit activity in the freely-moving rat. *Brain Res.* **34**, 171–175 (1971).
32. Hafting, T., Fyhn, M., Molden, S., Moser, M.B. & Moser, E.I. Microstructure of a spatial map in the entorhinal cortex. *Nature* **436**, 801–806 (2005).
33. Hargreaves, E.L., Rao, G., Lee, I. & Knierim, J.J. Major dissociation between medial and lateral entorhinal input to dorsal hippocampus. *Science* **308**, 1792–1794 (2005).
34. Lee, A.K. & Wilson, M.A. A combinatorial method for analyzing sequential firing patterns involving an arbitrary number of neurons based on relative time order. *J. Neurophysiol.* **92**, 2555–2573 (2004).
35. Steriade, M., Nubez, A. & Amzica, F. A novel slow (<1 Hz) oscillation of neocortical neurons *in vivo*: depolarizing and hyperpolarizing components. *J. Neurosci.* **13**, 3252–3265 (1993).
36. Steriade, M. & Amzica, F. Slow sleep oscillation, rhythmic K-complexes, and their paroxysmal developments. *J. Sleep Res.* **7** (suppl. 1): 30–35 (1998).
37. Achermann, P. & Borbely, A.A. Low-frequency (<1 Hz) oscillations in the human sleep EEG. *Neuroscience* **81**, 213–222 (1997).
38. Hahn, T.T.G., Sakmann, B. & Mehta, M.R. Phase-locking of hippocampal interneurons' membrane potential to neocortical up-down states. *Nat. Neurosci.* **9**, 1359–1361 (2006).
39. Kosslyn, S.M. *et al.* The role of area 17 in visual imagery: convergent evidence from PET and rTMS. *Science* **284**, 167–170 (1999).
40. Wheeler, M.E., Petersen, S.E. & Buckner, R.L. Memory's echo: vivid remembering reactivates sensory-specific cortex. *Proc. Natl. Acad. Sci. USA* **97**, 11125–11129 (2000).
41. Harris, J.A., Petersen, R.S. & Diamond, M.E. The cortical distribution of sensory memories. *Neuron* **30**, 315–318 (2001).
42. Suzuki, W.A. Encoding new episodes and making them stick. *Neuron* **50**, 19–21 (2006).
43. McClelland, J.L. & Goddard, N.H. Considerations arising from a complementary learning systems perspective on hippocampus and neocortex. *Hippocampus* **6**, 654–665 (1996).
44. O'Reilly, R.C. & Rudy, J.W. Computational principals of learning in the neocortex and hippocampus. *Hippocampus* **10**, 389–397 (2000).
45. Lavenex, P. & Amaral, D.G. Hippocampal-neocortical interaction: a hierarchy of associativity. *Hippocampus* **10**, 420–430 (2000).
46. Rolls, E.T. Hippocampal-cortical and cortico-cortical backprojections. *Hippocampus* **10**, 380–388 (2000).
47. Paxinos, G. & Watson, C. *The Rat Brain in Stereotaxic Coordinates* 4th edn. (Academic, New York, 1998).
48. Robert, C., Guilpin, C. & Limoge, A. Automated sleep staging systems in rats. *J. Neurosci. Methods* **88**, 111–122 (1999).
49. Siapas, A.G., Lubenov, E.V. & Wilson, M.A. Prefrontal phase locking to hippocampal theta oscillations. *Neuron* **46**, 141–145 (2005).
50. Skaggs, W.E., McNaughton, B.L., Gothard, K.M. & Markus, E.J. An information-theoretic approach to deciphering the hippocampal code. In *Advances in Neural Information Processing Systems* Vol. 5 (eds. Hanson, S.J., Cowan, J.D. & Giles, C.J.) 1030–1037 (Morgan Kaufmann, San Mateo, California, USA, 1993).

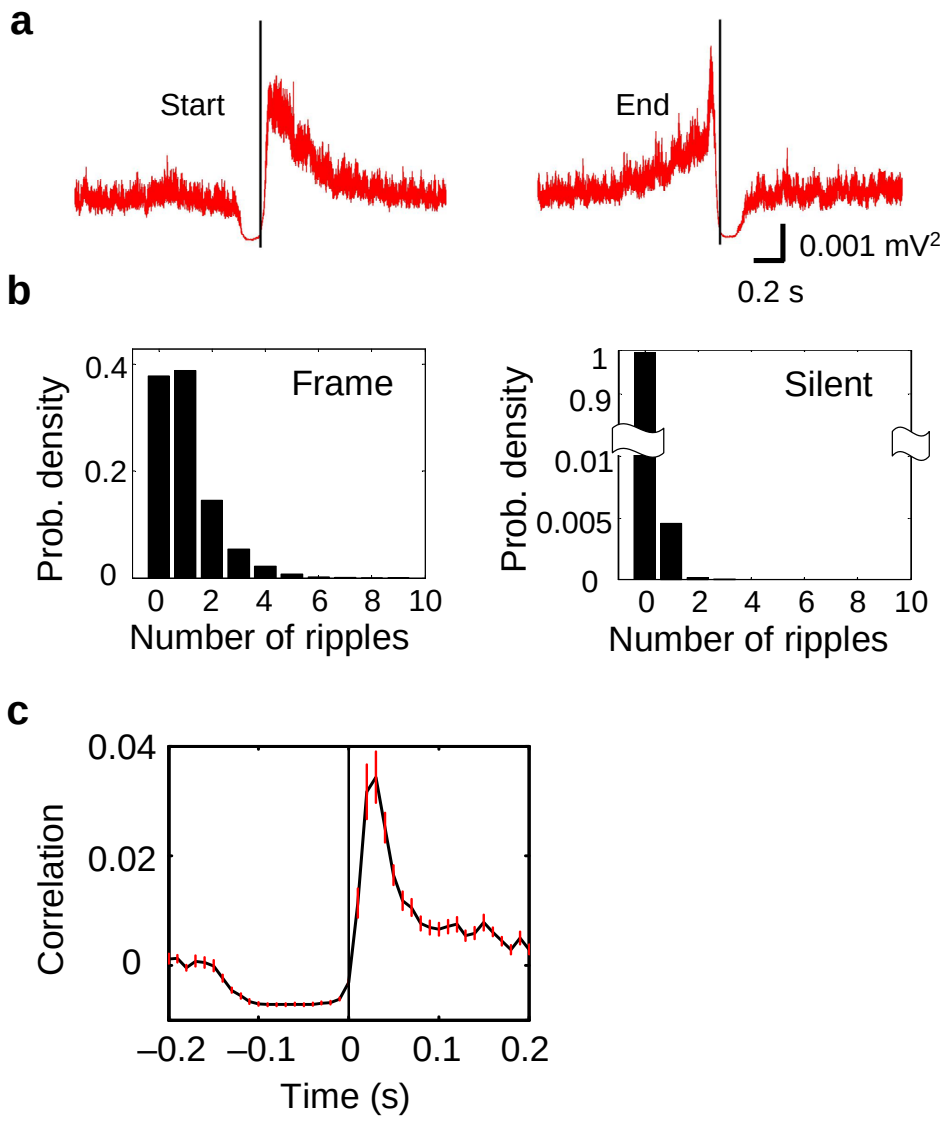

Supplementary Fig. 1 Hippocampal frames were related to hippocampal EEG ripples. (**a**) Hippocampal frame start time (Start) and end time (End) triggered averages of hippocampal EEG ripple power (mean ± s.e., as s.e. represented by the thickness of the curves). Hippocampal ripple power was significantly reduced immediately before the hippocampal frames started and immediately after they ended (that is, during the silent periods). (**b**) Distribution of number of ripple events contained within individual hippocampal frames and within inter-frame silent periods. Note y-axis in Between is truncated. (**c**) Average cross-correlogram (mean ± s.e., N = 20 sleep sessions) between hippocampal frame start times and ripple event start times. Hippocampal frame was reference. Bin size: 10 ms. P = 0.0000086 for the positive peak at 30 ms (t-test).

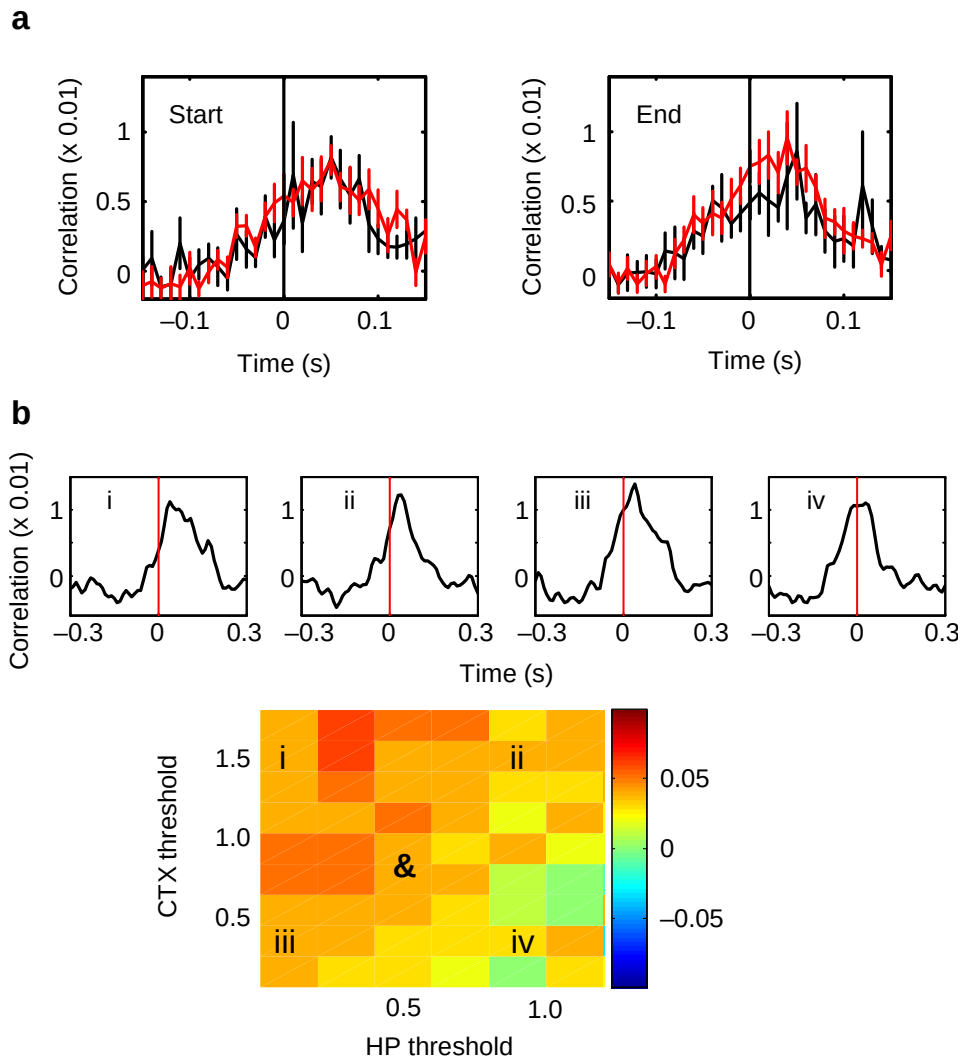

Supplementary Fig.2 Temporal relationship between cortical and hippocampal frames were not significantly different between PRE and POST, and were not sensitive to frame definition parameters. (**a**) Average (mean ± s.e, N = 20 sleep sessions) cross-correlograms between cortical and hippocampal frame start times (Start) and between their end times (End) during PRE (black) and POST (red). Here the cortex was the reference, meaning a peak at a positive time would indicate the cortex leads the hippocampus. Bin size: 10 ms. There was no significant difference between PRE and POST at each time lag for either Start ($P \geq 0.12$, paired t-test) or End ($P \geq 0.11$). (**b**) Peak times of cross-correlograms between cortical and hippocampal frame end times in a sleep session, given different thresholds (see **Supplemental Fig.12** for details) to define cortical (CTX) and hippocampal (HP) frames. For a wide range of thresholds, the peak of the cross-correlogram appeared at 20–60 ms. The peak shifted to negative only if hippocampal threshold was too large. Examples (i–iv) of cross-correlograms at different parameters are shown on top. &: actual parameters used in the analysis.

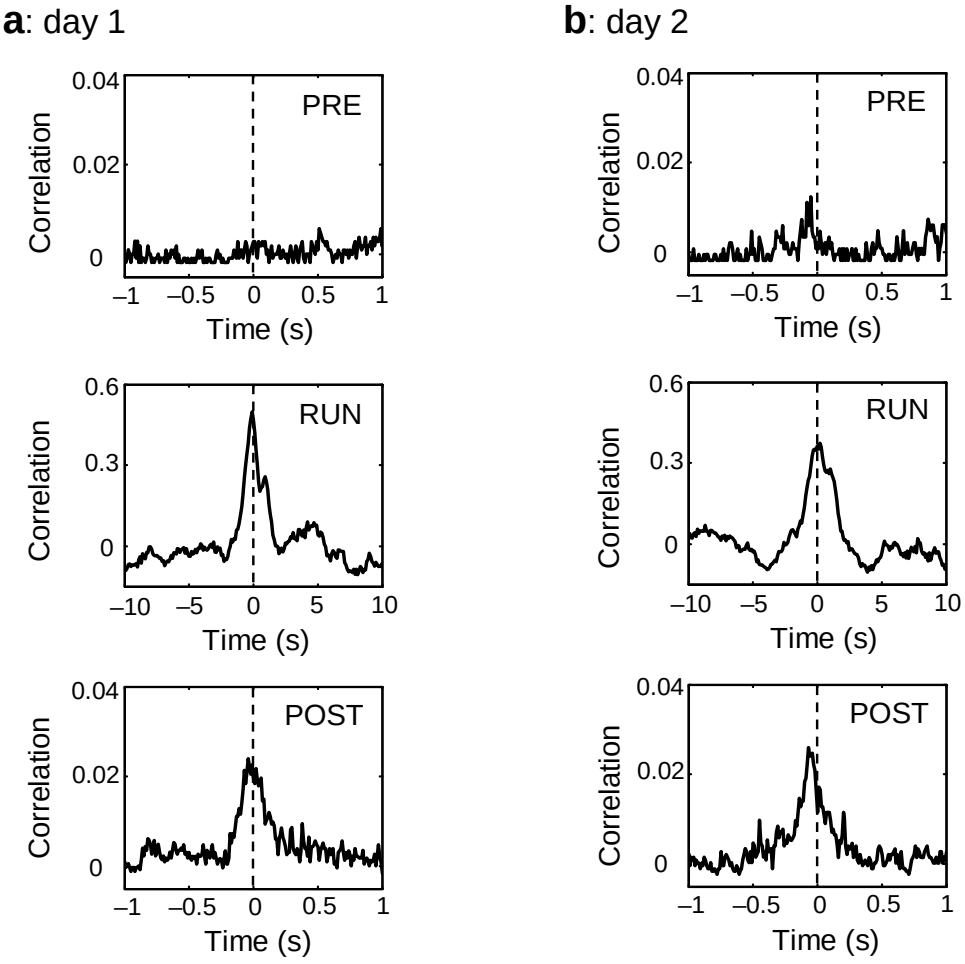

Supplementary Fig. 3 Cell pairs between the visual cortex and hippocampus that had high correlation during RUN also had high correlation in POST, but not in PRE. (**a**, **b**) Cross-correlograms between a visual cortical cell and a hippocampal cell during PRE, RUN, and POST for two consecutive recording days (**a**: day 1, **b**: day 2). The cortical cell was the reference, meaning a positive peak indicates the hippocampal cell follows the cortical cell. The two cells shown here are the same as in **Fig.3** in the main text. Bin size: 10 ms for PRE and POST; 100 ms for RUN. Dashed lines mark the time 0 lag. The cell pair had high correlation during RUN because they had overlapping firing fields (see **Fig.3** in the main text). The cell pair were more correlated during POST than during PRE. This effect was repeatable across the two days.

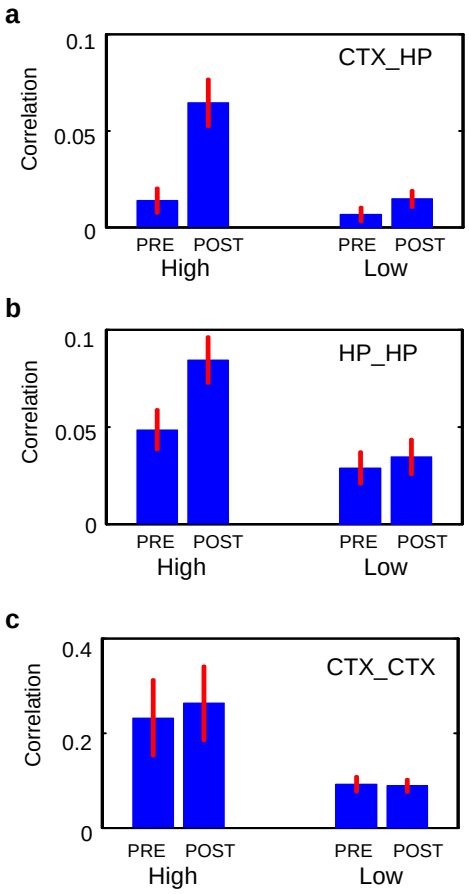

Supplementary Fig. 4 High but not low correlation during RUN boosted correlation in POST between the visual cortex and hippocampus, and within the hippocampus. Cell pairs were classified into a High group with run correlation ≥ 1 and a Low group with run correlation ∈ [-0.1, 0.1]. Correlation here was computed as sum of center 21 lags of a cross-correlogram (**Supplemental Fig.10** online). (**a**) Average correlation of the High and Low groups in PRE and POST sleep sessions for pairs between the cortex and hippocampus. (**b**, **c**) Same as **a**, but for pairs within the hippocampus (**b**) and within the visual cortex (**c**). The numbers of cell pairs (*N*) and *P* values (paired *t*-test) for PRE/POST comparisons are: (**a**) High: $N = 77$, $P = 0.00035$; Low: $N = 108$, $P = 0.16$; (**b**) High: $N = 58$, $P = 0.025$; Low: $N = 54$, $P = 0.64$; (**c**) High: $N = 48$, $P = 0.79$; Low: $N = 44$, $P = 0.88$. Note that correlations between cortical pairs were already high during PRE and the increase from PRE to POST was small. This can be explained by the cortical frame structure and cortical cells' high firing rate, which cause cortical cell pairs often participate in same frames and therefore high baseline correlation. Therefore, the low level pair-wise analysis is confounded by overall firing patterns, and not specific enough to detect memory-related change in fine firing patterns in the cortex.

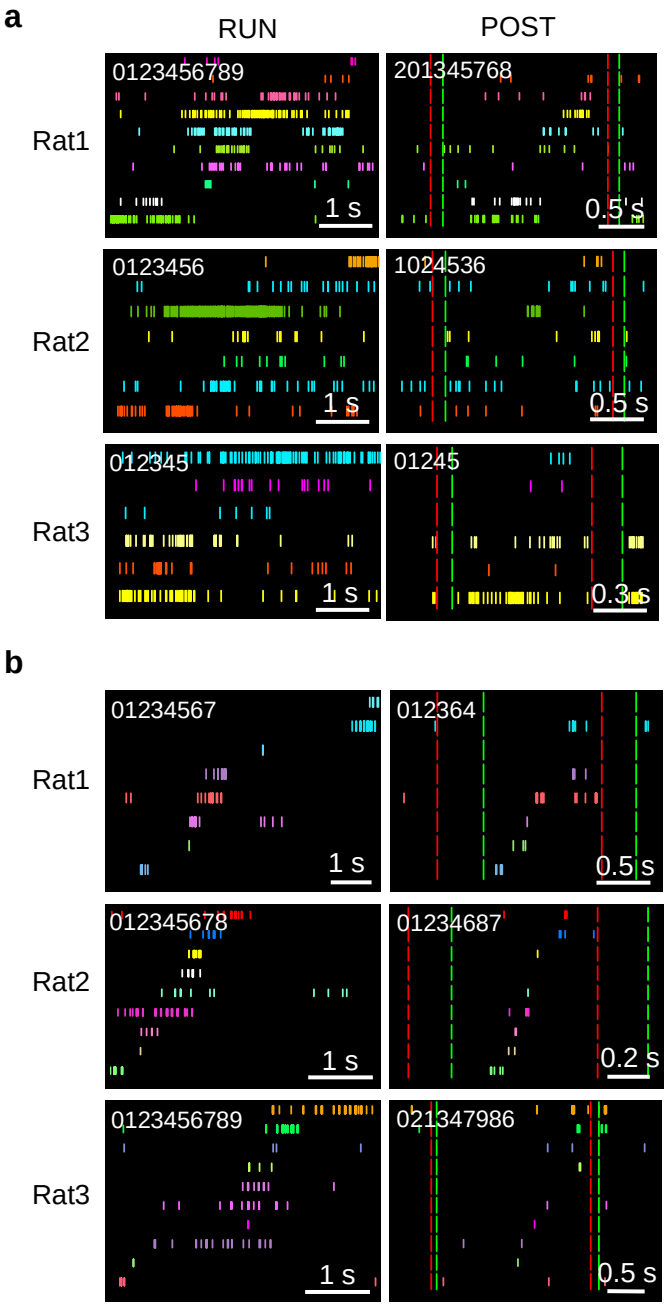

Supplementary Fig. 5 Firing patterns in the visual cortex (**a**) and hippocampus (**b**) during RUN were replayed in sleep frames during POST. Examples of firing patterns were taken from each of 3 rats (Rat1, Rat2, Rat3). In each panel, each row represents a cell and each tick represents a spike. The same cells are plotted for both RUN and POST. Run patterns were evoked when the rat ran a single lap on a trajectory. In POST, dashed green and red lines mark frame start and end times, respectively. The firing sequence during RUN (e.g. 0123456789) or in the frame (e.g. 201345768) is shown on top of each panel. The sequence matching probabilities for the POST frames are: (**a**) p = 0.00043, 0.015, 0.0083 for Rat1, Rat2, Rat3, respectively; (**b**) p = 0.0083, 0.0002, 0.0029 for Rat1, Rat2, Rat3, respectively.

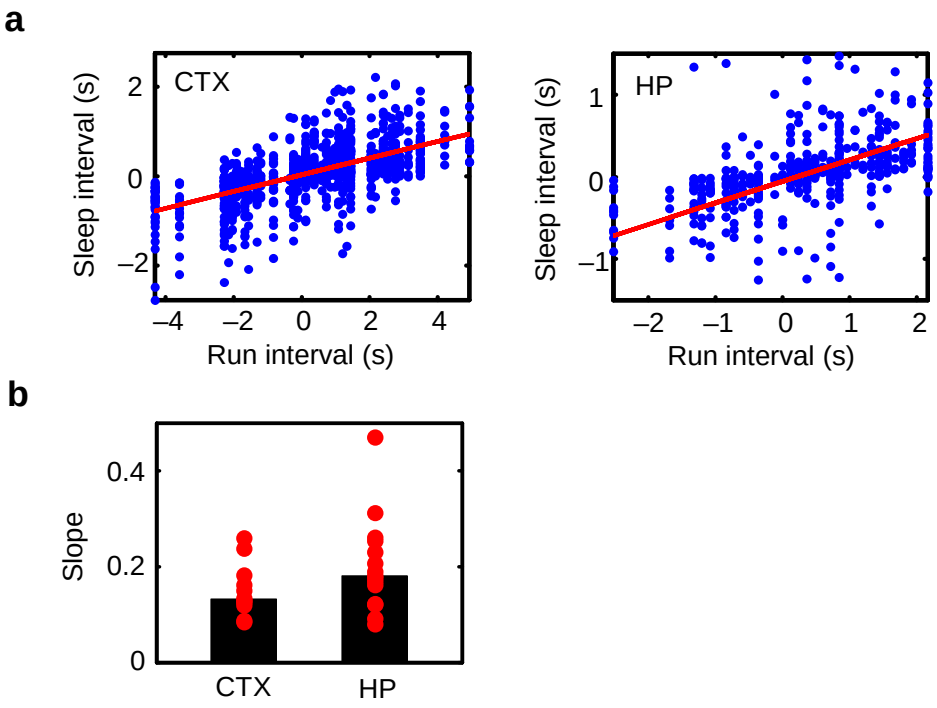

Supplementary Fig. 6 Frame replays were compressed during sleep. (**a**) Intervals between cell pairs in replaying sleep frames compared with their intervals on a trajectory during RUN in the cortex (CTX) and in the hippocampus (HP). Between a cell pair, RUN interval was defined as temporal distance between their peak firing times in a RUN template, while sleep interval in a frame defined as temporal distance between their peak firing times within the frame. Each blue dot represents one sleep interval in one replaying frame between one pair of cells and their corresponding RUN interval. The red lines are linear regressions between the sleep and RUN intervals. The slope of the regression gives the inverse of the compression factor for the trajectory. The slopes are 0.19 and 0.26 for CTX and HP, respectively. (**b**) Regression slopes for all trajectories in the cortex (CTX) and in the hippocampus (HP). Each red dot represents one trajectory. The numbers of total trajectories are 12 for CTX and 15 for HP. The black bars indicate the median value (0.13 for CTX, 0.18 for HP).

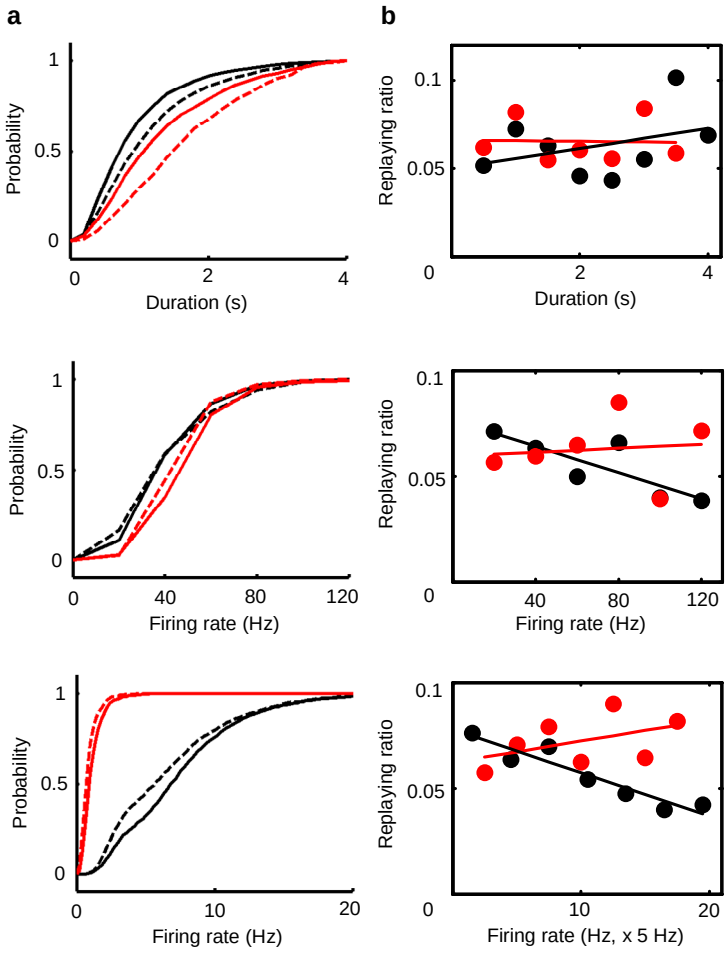

Supplementary Fig. 7 Difference in frame properties did not significantly contribute to increase in replaying ratio from PRE to POST. (**a**) Difference between PRE (broken lines) and POST (solid lines) in distribution of candidate frame duration (top), within-frame multiunit firing rate per tetrode (middle), and within-frame RUN-active cell firing rate (bottom) in the cortex (black) and hippocampus (red). The ranksum test *P* values for PRE/POST comparisons are: (top) CTX: 0, HP: 0; (middle) CTX: 0.22, HP: 0.0043; (bottom) CTX: 1.4×10^{-26}, HP: 6.3×10^{-23}. (**b**) Dependence of replaying ratio on frame duration (top), within-frame multiunit firing rate per tetrode (middle), and within-frame RUN-active cell firing rate (bottom) in the cortex (black) and hippocampus (red). Note that the hippocampal firing rates (red) in bottom are rescaled by 5x. Replaying and candidate frames in PRE and POST were combined and then grouped according their frame properties. Replaying ratios were computed as number of replaying frames divided by number of candidate frames in each group. Straight lines are linear regressions between the replaying ratios and the frame parameters. The *P* values (Pearson's *r*) for the linear correlations are: (top) CTX: 0.37, HP: 0.94; (middle) CTX: 0.040, HP: 0.85; (bottom) CTX: 0.0013, HP: 0.29. The only significant correlations here are the negative correlations between the replaying ratio and either the within-frame multiunit or RUN-active cell firing rate in the cortex. However, there was no change in multiunit rate and an increase in active cell rate from PRE to POST in the cortex. Therefore, the overall increase in replaying ratio from PRE to POST could not be explained by the difference in these parameters.

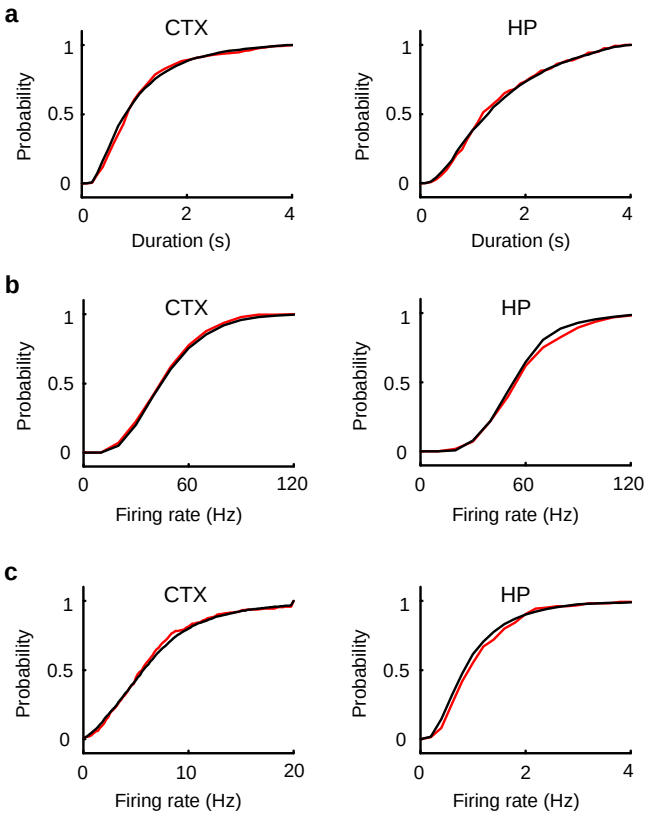

Supplementary Fig. 8 There were no significant differences in distribution of frame duration (**a**), within frame multiunit firing rate per tetrode (**b**), and within frame active cell firing rate (**c**) between replaying (red) and non-replaying (black) candidate frames in either the visual cortex (CTX) or the hippocampus (HP). The ranksum test *P* values are: (a) CTX: $P = 0.23$, HP: $P = 0.92$; (b) CTX: $P = 0.30$; HP: $P = 0.21$; (c) CTX: $P = 0.59$, HP: $P = 0.13$.

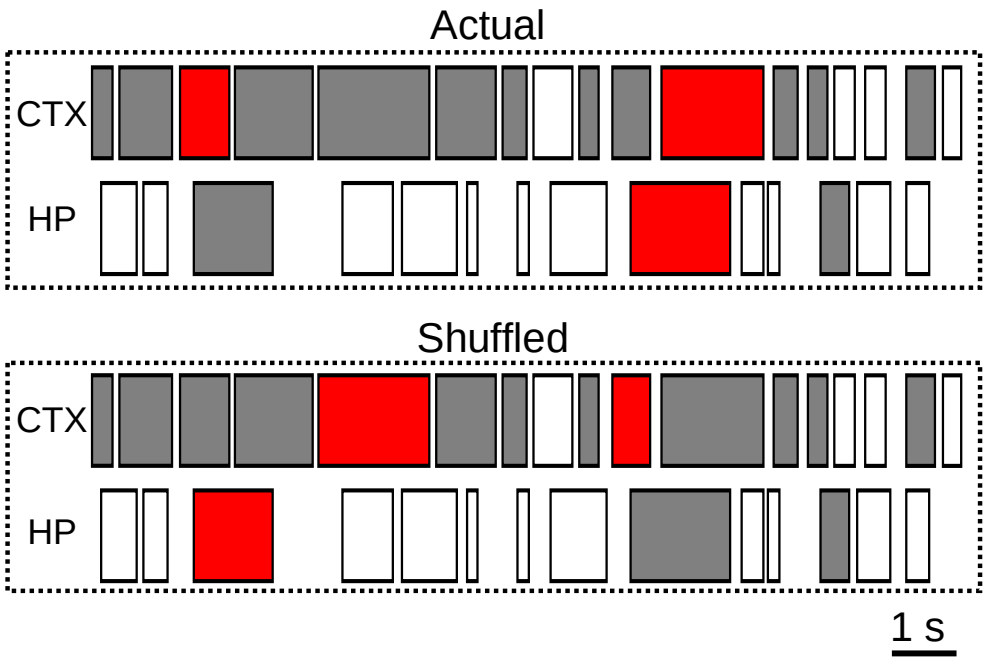

Supplementary Fig. 9 Shuffling procedure to determine significance (*P* value) of the overlapping replaying frame pairs. The replaying frames here are defined as matching probability $p < 0.05$. Cortical (CTX) and hippocampal (HP) frames within a 15 s SWS episode are displayed. Broken, gray, and red boxes represent non-candidate (active cell number < 4), candidate (active cell number ≥ 4), and replaying frames, respectively. A shuffled configuration (Shuffled) is generated from the actual configuration (Actual) by randomly re-distributing replaying frames (red) among all the candidate (gray) frames in the entire SWS session.

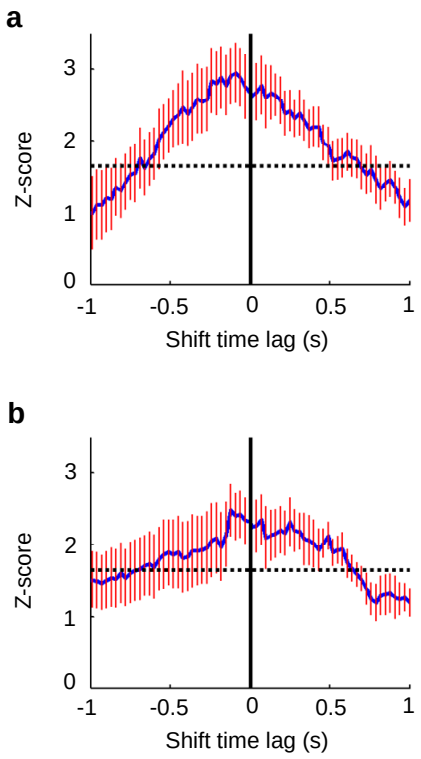

Supplementary Fig. 10 Temporal relationship between cortical and hippocampal sequence replays. Average (mean ± s.e.) Z-scores of match indices between cortical and hippocampal cell pairs, based on cortical (**a**) and hippocampal (**b**) replaying frames, are plotted with respect to relative time shift between cortical and hippocampal frames. As in the interval analysis, we took all the cortical frames that replayed a trajectory and their overlapping hippocampal frames (**a**). We then paired cells across the two areas within those frames. Let *m* be the number of pairs that had the same firing order within a cortical replaying frame and its overlapping hippocampal frame as during RUN template, and *n* the number of pairs with the opposite order. Similar to the case of cell pairs within same area, match index here is defined as $I = (m-n)/(m+n)$. We then randomly shuffled cell identities in the cortical template and re-calculated the match index 1000 times. Z-score of the observed match index was computed against the distribution of the shuffling-generated match indices. We then shifted the cortical replaying frames against their overlapping hippocampal frames and computed the match index Z-score for each shift time. Dotted line indicates Z-score significance level at 0.05. The curve is averaged Z-score over 11 trajectories from 4 rats. The broad peak at negative shift time lag means that the match index was larger when cortical frames were shifted to the left (earlier time), suggesting hippocampal replays might lead cortical replays. Similarly we also did the analysis based on all the hippocampal replaying frames and their overlapping cortical frames (**b,** $N = 10$ trajectories from 3 rats). Here a positive peak would mean hippocampal replay occurred earlier than the cortical replay. In this case, the peak is even broader and the location of the peak is not clear. The overall result suggests a trend toward the hippocampus leading the cortex during replay. However, the data did not amount to a definitive conclusion regarding the temporal relationship between cortical and hippocampal replays.

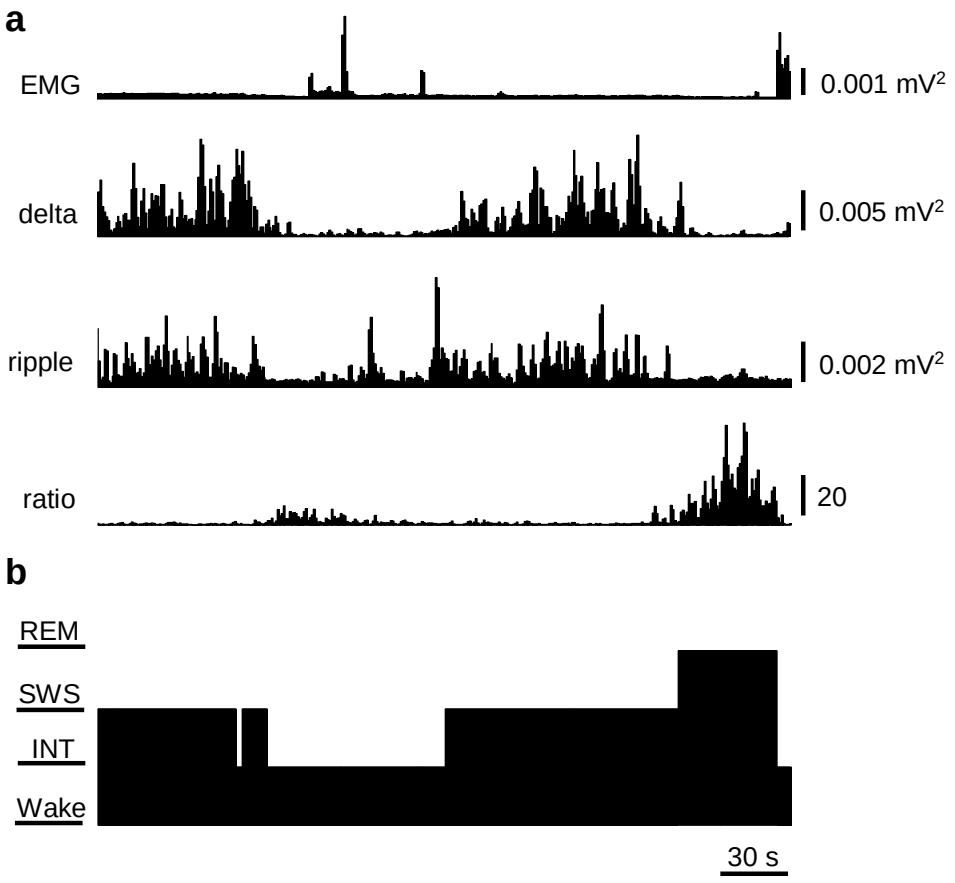

Supplementary Fig. 11 Sleep stage classification. (**a**) Power of EMG, cortical EEG at delta band (delta), hippocampal EEG at ripple band (ripple), and power ratio of hippocampal EEG theta to delta (ratio) during a 6-minute sleep episode. (**b**) The same sleep period was classified into different states at 1 s resolution: awake state (Wake), slow-wave sleep (SWS), rapid eye movement sleep (REM), and unspecified intermediate state (INT).

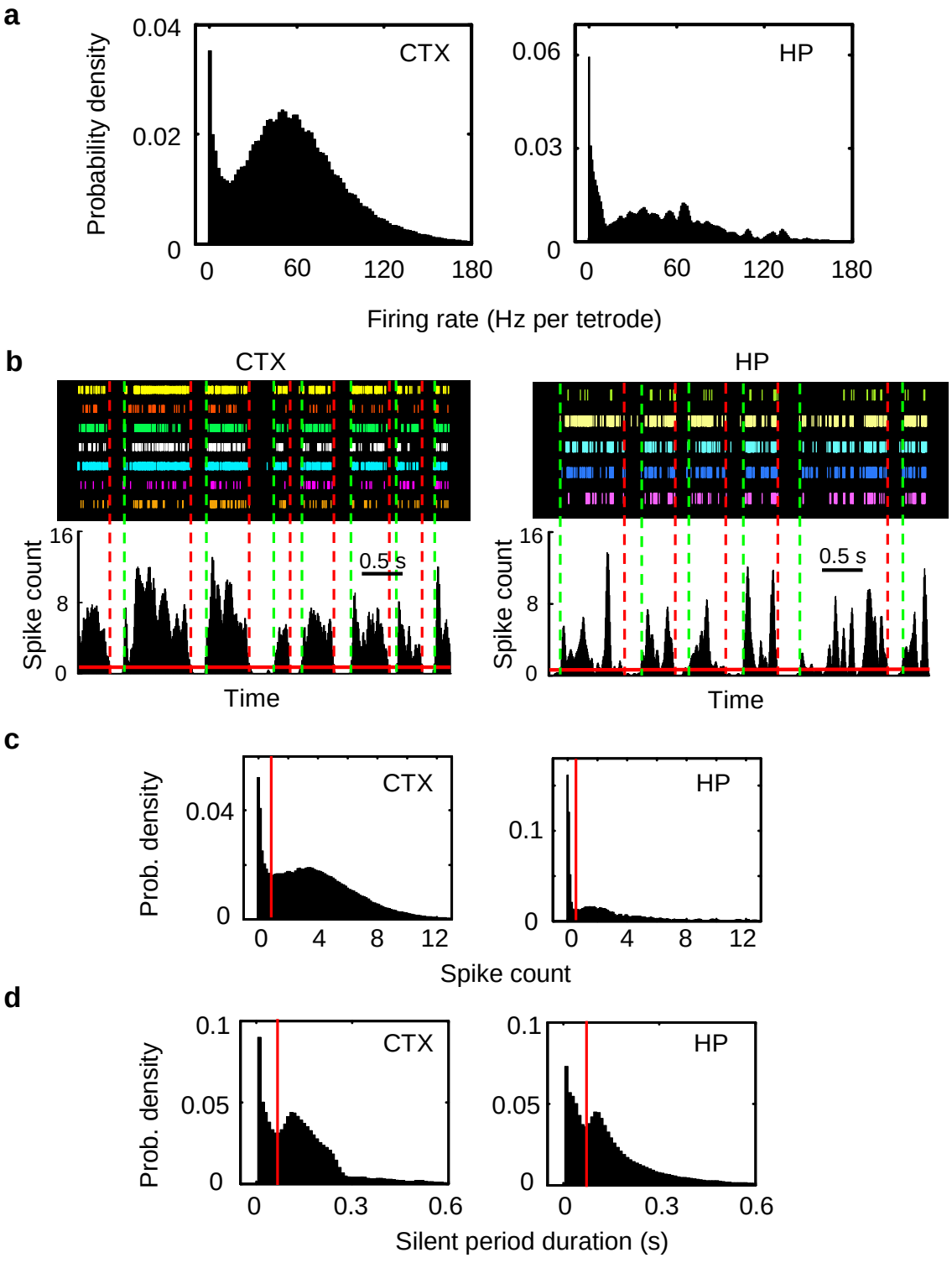
a
Probability density
0.04
0.02
0
CTX
0
60
120
180
0.06
0.03
0
HP
0
60
120
180
Firing rate (Hz per tetrode)
b
CTX
HP
Spike count
16
8
0
0.5 s
Time
c
Prob. density
0.04
0
CTX
0
4
8
12
0.1
0
HP
0
4
8
12
Spike count
d
Prob. density
0.1
0.05
0
CTX
0
0.3
0.6
HP
Silent period duration (s)

Supplementary Fig. 12 Frame boundary determination.
(**a**) Bimodal distribution of multiunit firing rates in the visual cortex (CTX: binsize = 100 ms, N = 20 sleep sessions) and hippocampus (HP: binsize = 200 ms, N = 20 sleep sessions). The sharp peak at 0 indicates that there were many time bins when the entire neuronal population was silent, indicating the existence of the alternating frame and silence structure at the corresponding time scale.

(**b**) Frames were defined from binned multiunit spike count. Top panels show all the multiunit spikes during a SWS episode in the visual cortex (CTX) and in the hippocampus (HP). Each tick represents a spike and each row includes all the spikes recorded from a tetrode. It can be seen that the transitions between frames and silent periods were much faster than the time scale of silent periods. To determine the fast frame onsets and offsets at a fine time scale, spikes from all tetrodes were counted within 10ms bins and then smoothed with a 30 ms Gaussian window on the bottom. The smoothing was to prevent isolated spikes in silent periods from being classified as frames. A spike count threshold (T: red solid lines) was determined from the spike count distribution (see below **c**). The threshold crossing time points were assigned to either frame start times (green vertical dashed lines) or end times (red vertical dashed lines). Second, if the time gap between an end time and the following start time was shorter than a frame gap threshold (G), the two frames were merged.

(**c**) The spike count threshold (T) was determined from distribution of spike counts with 10 ms bins in both the visual cortex (CTX) and hippocampus (HP). The large peaks at zero indicate many bins were silent. The idea was to find a spike count value that separated active bins from silent bins. Note that spike count could take continuous values since we smoothed the spike count curve. Besides bins with 0 spike count, we also considered those time bins with small number of spikes and surrounded by silent bins (therefore a small spike count value after smoothing) as silent. The threshold (red vertical line) was defined as the spike count value at which the distribution reached its first minima.

(**d**) Similarly, minimum frame gap (G) (red vertical line) was determined from distribution of silent period durations in both the visual cortex (CTX) and hippocampus (HP). The peak at 10ms indicates short breaks within frames and the second peak (> 100 ms) indicates peak duration of inter-frame silent periods.

Since the recorded multiunit activity per tetrode varied from animal to animal, the spike count thresholds and minimum frame gaps were slightly different across animals (animal 1, CTX: T = 0.8 , G = 80 ms; HP: T = 0.6, G = 90 ms. animal 2, CTX: T = 0.8, G = 70 ms; HP: T = 0.5, G = 70 ms. animal 3, CTX: T = 0.8, G = 80 ms; HP: T = 0.8, G = 90 ms. animal 4, CTX: T = 0.8, G = 70 ms; HP: T = 0.5, G = 80 ms).

Supplementary Table 1. Minimum matching indices (I) required for significant frame sequences, given the number of cells in a frame (M). The corresponding matching probability (p), number of same order cell pairs (m) and number of opposite order cell pairs (n) are also shown. The threshold for a frame sequence to be significant is $p < 0.05$. The exact cutoff threshold for significant sequences with a particular M is given in the column of matching probability p (red). For $M \leq 3$, no sequences are significant.

Cell Number (M)	Matching Index (I)	Matching Probability (p)	Number of same order pair (m)	Number of opposite order pair (n)
4	1	0.042	6	0
5	0.8	0.042	9	1
6	0.73	0.028	13	2
7	0.62	0.035	17	4
8	0.57	0.031	22	6
9	0.50	0.038	27	9
10	0.47	0.036	33	12
11	0.42	0.043	39	16
12	0.39	0.041	46	20
13	0.36	0.049	53	25
14	0.34	0.047	61	30
15	0.33	0.045	70	35

Supplementary Table 2. Comparison in replaying frame ratio between PRE and POST in the visual cortex for each of the 12 trajectories.

			PRE			POST		
Animal	Date	Trajectory	Number of candidate frames	Number of replaying frames	Replaying ratio	Number of candiate frames	Number of replayign frames	Replaying ratio
		All	3070	163	0.0531	5808	366	0.0630
Rat 1	7/10/03	leftright	88	3	0.0341	289	17	0.0588
		rightleft	22	0	0	145	14	0.0966
	7/12/03	leftright	353	21	0.0595	283	20	0.0707
		rightleft	343	26	0.0758	243	21	0.0864
	7/13/03	leftright	118	6	0.0508	173	13	0.0751
		rightleft	211	15	0.0711	303	22	0.0726
Rat 2	12/15/03	leftright	499	9	0.0180	1355	41	0.0303
	12/16/03	leftright	240	6	0.0250	1234	58	0.0470
		rightleft	111	12	0.1081	583	82	0.1407
Rat 3	12/12/04	leftright	413	22	0.0533	703	47	0.0669
Rat 4	10/25/03	leftright	313	20	0.0639	263	10	0.0380
	10/26/03	leftright	359	23	0.0641	234	21	0.0897
				Mean	0.0520		Mean	0.0727
				S.E.	0.0084		S.E.	0.0086

Supplementary Table 3 Comparison in replaying frame ratio between PRE and POST in the hippocampus for each of the 15 trajectories.

			PRE			POST		
Animal	Date	Trajectory	Number of candidate frames	Number of replaying frames	Replaying ratio	Number of candiate frames	Number of replayign frames	Replaying ratio
		All	849	39	0.0459	1555	121	0.0778
Rat 1	7/10/03	rightleft	28	0	0	52	2	0.0385
	7/12/03	leftright	21	1	0.0476	17	1	0.0588
		rightleft	103	3	0.0291	91	9	0.0989
	7/13/03	leftright	127	7	0.0551	163	9	0.0552
		rightleft	23	4	0.1739	47	6	0.1277
Rat 2	12/14/03	leftright	59	2	0.0339	115	10	0.0870
		rightleft	61	3	0.0492	110	12	0.1091
	12/15/03	leftright	90	2	0.0222	303	21	0.0693
		rightleft	16	1	0.0625	73	9	0.1233
	12/16/03	leftright	24	2	0.0833	110	8	0.0727
		rightleft	23	0	0	69	3	0.0435
Rat 3	12/11/04	leftright	90	3	0.0333	142	11	0.0775
		rightleft	107	7	0.0654	127	10	0.0787
	12/12/04	leftright	54	4	0.0741	93	6	0.0645
		rightleft	23	0	0	43	4	0.0930
				Mean	0.0486		Mean	0.0798
				S.E.	0.0113		S.E.	0.0069

Supplementary Methods

Template sequence construction

The entire RUN session was divided into individual running laps. Laps were grouped into one of the two trajectories (leftright and rightleft). First, the two trajectories were linearized, and we computed a spatial firing rate curve $f_i(i = 1,2,...,n)$ for a cell at each spatial bin *i* (2 cm) on a linearized trajectory. Firing rate at a spatial bin was defined as number of spikes divided by total occupancy time in the bin. Secondly, the spatial firing rate curve was then transformed to a temporal firing rate curve $f(t)$, by converting each position point *i* to its average occupancy time during a single lap. The peak of the curve was taken as the cell's firing time on the trajectory. Visual cells often had one or more fields, therefore one or more firing peaks. In this case, we used the dominant peak. Numbers (0, 1, …) were assigned to the cells and were arranged to form a template sequence according to the order of the cells' relative firing times. In order for a cell to be included in a template, first, the cell had to be active on the trajectory and had high spatial information (> 0.8 bit spike^{-1}). Moreover, the cell had to have a stable dominant field, qualified as its peak firing locations in at least 70% of the laps occur at the same place as the peak of its average firing rate curve (see below for how to determine peak firing time of a single spike train). For each trajectory on each recording day, one hippocampal and one cortical template sequence could be constructed. Only template sequences with at least 5 cells were included in the analysis. As a result, a total of 12 (out of 20 possible) cortical template sequences and 15 (out of 20 possible) hippocampal template sequences were analyzed from 10 recording days in 4 rats.

Frame sequence construction

For each frame, we first assigned the same letters as in a template sequence to cells that were also active in the frame. Then we ordered the letters according to their relative firing times in the frame. We defined a cell's firing time in a frame as the time when its firing reaches its maximum. To determine the maximum firing time of a single spike train $\{t_1, t_2, ..., t_n\}$, where t_i is the *i*-th spike's time, we convolved each spike with a Gaussian kernel to create an (unnormalized) instantaneous firing rate curve as a function of time *t*:

$$f(t) = \sum_{i=1}^{n} k(t - t_i, \sigma),$$

where the Gaussian kernel $k(t,\sigma)$ is,

$$k(t,\sigma) = \frac{1}{\sigma\sqrt{2\pi}} e^{\frac{-t^2}{2\sigma^2}}.$$

σ here is the smoothing window. The time at which *f(t)* takes the maximum was considered as the cell's firing time in the frame. In this study, σ = 180 ms was used for hippocampal and σ = 400 ms for cortical cells. Results were similar if $\sigma \in$ [50 250] ms was used for hippocampal cells and $\sigma \in$ [100 600] ms for cortical cells.

Sequence matching index and matching probability

Sequence matching index measures how similar a frame sequence matches a template sequence, and matching probability measures how significant the matching is. The method described here utilizes a similar combinatorial scheme as in Lee and Wilson (2004), but uses a different similarity measurement. Let *M* be the number of cells in a frame sequence. A total of *M(M-1)/2* cell pairs can be combined. If *m* is the number of pairs that have the same order in the frame as in the template and *n* the number of pairs with opposite order, we defined a matching index *I* as

$$I = (m - n)/(m + n) \ .$$

I is bounded in [-1 1]. If *I* = 1, the cells in the frame have the exact same order as in the template. If *I* = -1, the cells have exactly reverse order as in the template. Given a matching index I_0, we can ask how significant I_0 is, assuming a null hypothesis that cell orders are randomly arranged and all cell orders are equally possible. For this purpose, we can compute the matching probability *p*, defined as

$$p = \Pr ob\{I \geq I_0 \mid cell\# = M\} .$$

The probability is on the condition that *M* cells are present in a frame sequence.

For small *M* (< 11), all combinations of *M* cells were actually generated and the exact matching probabilities were computed. For an example, given a frame sequence 02546, we have *M* = 5 and *I* = (9-1)/(9+1) = 0.8. All the possible arrangements of the 5 cells are:

02456 02465 02645 06245 60245
……

06542 60542 65042 65402 65420

There are 120 possible combinations. The corresponding matching indices are:

1.0 0.8 0.6 0.4 0.2
……

-0.2 -0.4 -0.6 -0.8 -1.0

There are 5 combinations (02456, 20456, 04256, 02546, 02465) with a matching index equal to or larger than 0.8. Therefore, the matching probability for 02546 is *P* = 5/120 = 0.042.

For $M \geq 11$, the number of all possible combinations is too large to be generated, so we generated 10000 random samples, from which the matching probability was approximated. The *P* values for *M* up to 20 and for all possible matching indices were obtained.

Unless otherwise specified, we used a threshold $p < 0.05$ to mark a significant frame sequence and considered the frame as replaying. Due to the limited number of all possible combinations of *M* cells, *P* only takes discrete values (as shown in the example

above). The exact cutoff threshold is not exactly 0.05, but depends on *M*. For different *M*, the minimum matching indices required for a replaying sequence and the corresponding matching probabilities (therefore the corresponding cutoff threshold for replaying frames with cell number *M*) are listed in Supplementary Table.1 online. It is necessary that $M \geq 4$ for a frame to be considered replaying, since none of the frames with $M \leq 3$ can reach the significance threshold $p < 0.05$. Therefore, we did further analysis only for the frames with at least 4 active template cells and called them candidate frames. One sleep frame could be candidate frame for both the template sequences generated from the two running trajectories on the same day. In this case, we assigned the frame as candidate frame only for the template with the higher matching index.

Replay chance significance and shuffle significance

Given *K* candidate frames (since the probability that a non-candidate frame is replaying is 0, including non-candidate frames in the analysis produces exactly the same result) and if *L* replaying frames are observed, we computed how significantly different *L* is from number of randomly generated replaying frames. For this purpose, two null hypotheses were generated: (1) Each frame replays its template sequence independently with a probability the same as the corresponding cutoff threshold; (2) Each template is replayed with the same probability as its random shuffles. The first hypothesis is equivalent to the assumption that cells in each frame are arranged randomly and independently. The second is equivalent to assuming that cells are arranged randomly but keep their identities across all frames. The significance generated from the first hypothesis is called chance significance and the one from the second shuffle significance.

To test the first hypothesis, we computed the distribution of replaying frame number generated from the hypothesis. We first grouped all the candidate frames for all the templates according to their cell numbers.

$$K = K_4 + K_5 + K_6 + \ldots,$$

where K_i ($i \geq 4$ since candidate frames had a minimum 4 cells) is the number of frames with *i* active cells. The total number of replaying frames expected is the sum of replaying frames expected in each group.

$$L = L_4 + L_5 + L_6 + \ldots$$

For group *i*, the probability p_i that a frame in the group is replaying is given in Supplementary Table 1 online. According to the assumption that frames are independent of each other, L_i follows a binomial distribution with parameters p_i and K_i, which can be approximated by a Poisson distribution with parameter $p_i K_i$ because of the small p_i and large K_i. Furthermore, since sum of independent Poisson variables is still Poisson, *L* follows a Poisson distribution with parameter $\sum_i p_i K_i$. When $\sum_i p_i K_i$ is large (in this analysis it was > 30 for all trajectories combined), the Poisson distribution can be approximated by a normal distribution with mean,

$$a = \sum_i p_i K_i ,$$

and standard deviation

$$s = \sqrt{\sum_i p_i K_i} \ .$$

In the end, the chance significance was given by

$$P = \int_L^\infty \frac{1}{s\sqrt{2\pi}} e^{-\frac{(x-a)^2}{2s^2}} dx \ .$$

To compute shuffle significance, we first generated shuffled sequences by randomly permuting numbers in real templates. Then we counted how many frames out of the total *K* candidate frames that replayed the shuffled sequence with the same cutoff thresholds $p < 0.05$ as listed in **Supplementary Table 1** online. The shuffling was done for every template and the counts from all the templates were combined. The procedure was repeated for 1000 times. The normalized histogram of the 1000 counts gave rise to the shuffle distribution of replaying frame number. The shuffle significance *P* value was given as the number of shuffles that generated equal or more replaying frames than the actual observed number *L*, divided by total number of shuffles (i.e. 1000).

Overlapping replaying frame pairs and significance

Overlapping frame pairs were defined as one cortical frame and one hippocampal frame that share at least one time point in sleep. One frame could overlap with one or more frames in the other area. The significance of frame overlapping was evaluated by the following shuffling procedure (**Supplementary Fig.9** online). Given total K_h candidate frames and L_h replaying frames in the hippocampus and total K_c candidate frames and L_c replaying frames in the cortex, we randomly assigned any L_h of the K_h and any L_c of the K_c frames to be replaying. Then the overlapping replaying frame pairs for this assignment were counted. The shuffling was done for each of the 9 trajectories for which both cortical and hippocampal templates were available, and then combined. We repeated the procedure 1000 times and obtained the distribution of the number of overlapping replaying pairs. The significance (*P* value) was defined as number of shuffles that produced equal or more overlapping pairs than the actual observed number, divided by the total number of shuffles (i.e. 1000).

Interval analysis

RUN interval between two cells on a trajectory was the timing difference between peaks of their temporal firing rate curves on the trajectory. Sleep interval between two cells, each in a sleep frame, was the timing difference between peaks of their kernel-smoothed firing rate curves in the frames. For each cortical replaying frame for a trajectory, we took all hippocampal frames that overlap with the cortical frame. We paired up every cell in the cortical replaying frame with every cell in every overlapping hippocampal frame. Linear correlation coefficient between all sleep intervals belonging to a trajectory and their corresponding RUN intervals was computed. To control for the contribution of nonspecific factors to the correlation, we applied the following shuffling procedure. We randomly permuted cells in the cortical template for the trajectory and computed a shuffled copy of the RUN intervals. Then the correlation coefficient between the sleep

intervals and the shuffled RUN intervals was computed. The shuffling was done for 1000 times. The resulted distribution of the coefficient values was compared with the actual value to measure how significant the actual correlation was. The significance (*P* value) was given as the number of shuffles that produced equal or higher correlation coefficient than the actual value, divided by the total number of shuffles (i.e. 1000). The analysis was also done based on hippocampal replaying frames and their overlapping cortical frames.